Electronic Supplementary Material (ESI) for CrystEngComm.

Electronic Supplementary Information (ESI)

Extending the structural landscape of Mo(VI) hydrazonato inorganic-organic POM-hybrids: an experimental and computational study

Nikol Bebić,[a] Edi Topić,[a] Mirna Mandarić,[a] Tomica Hrenar,[a] and Višnja Vrdoljak*[a]

Contents

[a]University of Zagreb, Faculty of Science, Department of Chemistry, Horvatovac 102a, 10000 Zagreb, Croatia

List of compounds and designation scheme

Hexamolybdate-based hybrids

$[MoO_2(HL^1)(H_2O)]_2[Mo_6O_{19}]$ ($\mathbf{1^{Hw}}$)

$[MoO_2(HL^2)(MeCN)]_2[Mo_6O_{19}]\cdot 2MeCN$ ($\mathbf{2^{Hm}}\cdot$2MeCN)

$[MoO_2(HL^2)(MeCN)]_2[Mo_6O_{19}]\cdot 4MeCN$ ($\mathbf{2^{Hm}}\cdot$4MeCN)

$[Mo_2O_2(\mu\text{-}O)_2(HL^3)_2][Mo_6O_{19}]$ ($\mathbf{3^{H}}$)

$[MoO_2(HL^3)(H_2O)]_2[Mo_6O_{19}]$ ($\mathbf{4^{Hw}}\cdot$4MeCN)

Octamolybdate-based hybrids

$[MoO_2(HL^1)(H_2O)]_4[Mo_8O_{26}]\cdot 2MeCN\cdot 4H_2O$ ($\mathbf{1^{Ow}}\cdot$2MeCN$\cdot$4H_2O).

$[MoO_2(HL^2)(H_2O)]_4[Mo_8O_{26}]\cdot 2MeCN\cdot 10H_2O$ ($\mathbf{2^{Ow}}\cdot$2MeCN$\cdot$10H_2O).

$[MoO_2(H_2L^2)(H_2O)]_2[Mo_8O_{26}]\cdot 4MeCN\cdot 2H_2O$ ($\mathbf{2^{Ow\text{-}2}}\cdot$4MeCN$\cdot$2$H_2O$).

$[MoO_2(H_2L^4)(H_2O)]_2[Mo_8O_{26}]\cdot 2MeCN\cdot 3H_2O$ ($\mathbf{4^{Ow\text{-}2}}\cdot$2MeCN$\cdot$3$H_2O$).

$[MoO_2(H_2L^4)(H_2O)]_2[Mo_8O_{26}]\cdot 3MeCN\cdot 4H_2O$ ($\mathbf{4^{Ow\text{-}2}}\cdot$3MeCN$\cdot$4$H_2O$).

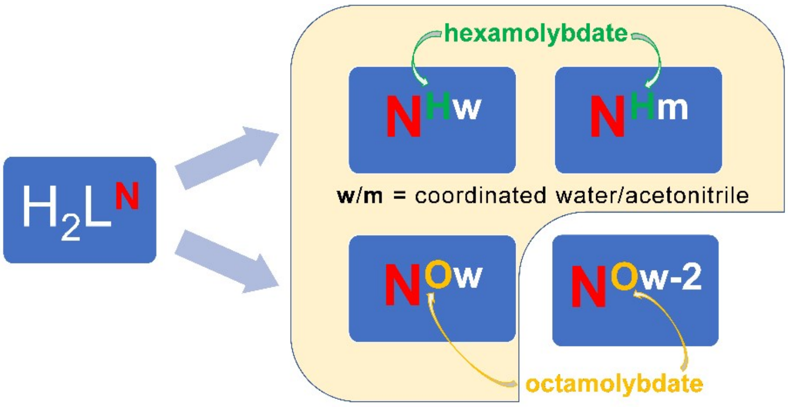

Scheme S1. Compounds designation scheme – **H** and **O** indicate hexamolybdate and octamolybdate anion, respectively. **w** and **m** denote coordinated water and MeCN molecules, respectively. Compounds **N**$^{\mathbf{Hw}}$, **N**$^{\mathbf{Hm}}$, **N**$^{\mathbf{Ow}}$ comprised ligand in HL^- form, whereas octamolybdates **N**$^{\mathbf{Ow\text{-}2}}$ comprised ligand in H_2L form.

Photos of different crystalline products

		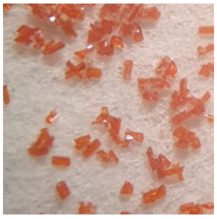
$\mathbf{1}$	$\mathbf{1^{Hw}}$	$\mathbf{1^{Ow}}\cdot 2\text{MeCN}\cdot 4\text{H}_2\text{O}$

(a)

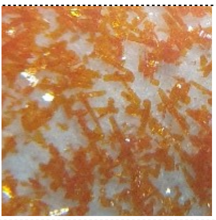	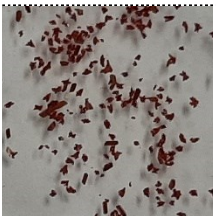	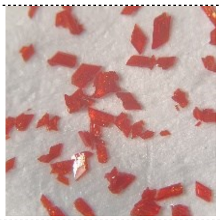	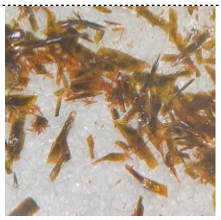
$\mathbf{2}$	$\mathbf{2^{Hm}}\cdot 4\text{MeCN}$	$\mathbf{2^{Ow}}\cdot 2\text{MeCN}\cdot 10\text{H}_2\text{O}$	$\mathbf{2^{Ow\text{-}2}}\cdot 4\text{MeCN}\cdot 2\text{H}_2\text{O}$

(b)

Figure S1. (a) Photos of different crystalline products with ligand H_2L^1. (b) Photos of different crystalline products with ligand H_2L^2. The solvates are unstable and lose solvent molecules.

IR-ATR and NMR spectra of polynuclear and mononuclear byproducts

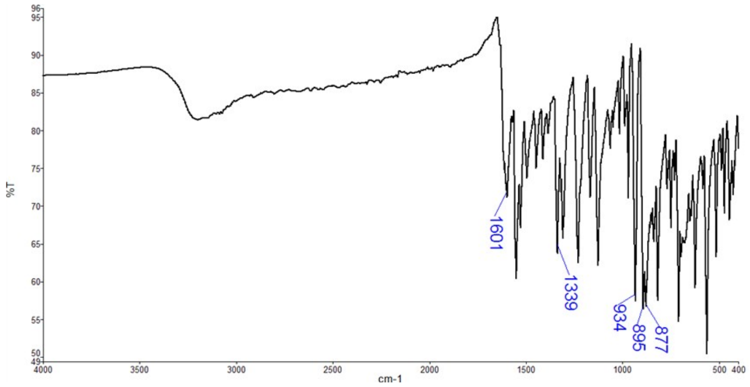

$[MoO_2(L^2)]_n$

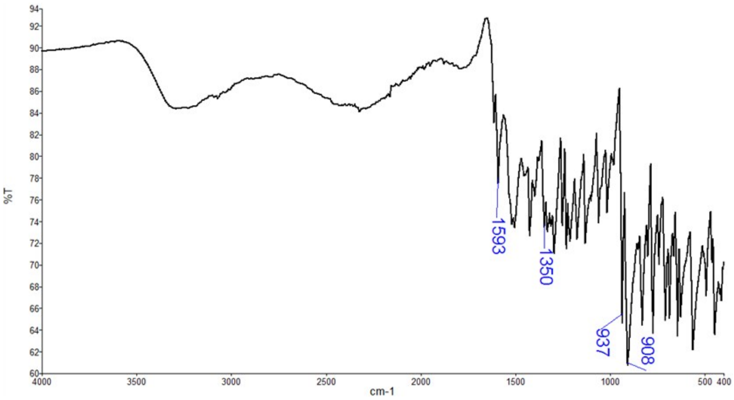

$[MoO_2(L^2)(H_2O)]$

Figure S2. Representative IR-ATR spectra of byproducts $[MoO_2(L^2)]_n$ and $[MoO_2(L^2)(H_2O)]$

.

For **1**-**4** complexes ^{1}H, ^{13}C-APTq NMR spectra were recorded on Bruker Avance III HD 400 MHz/54 mm Ascend spectrometer equipped with a 5 mm PA BBI 1H/D-BB Z-GRAD probe head. Representative examples are given in Figures S3 and S4.

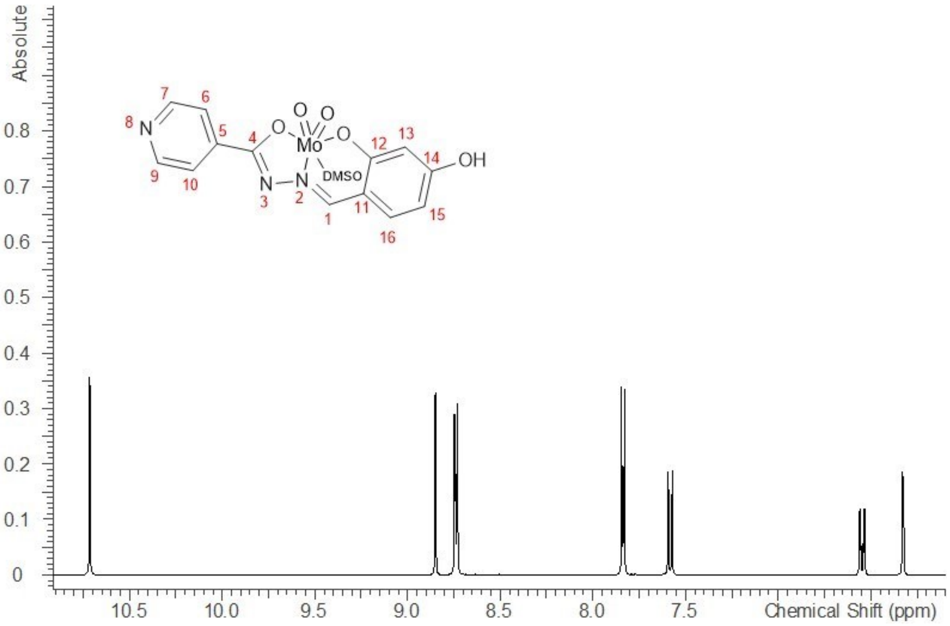

Figure S3. Representative ^{1}H NMR spectra of **2** in dmso-d_6.

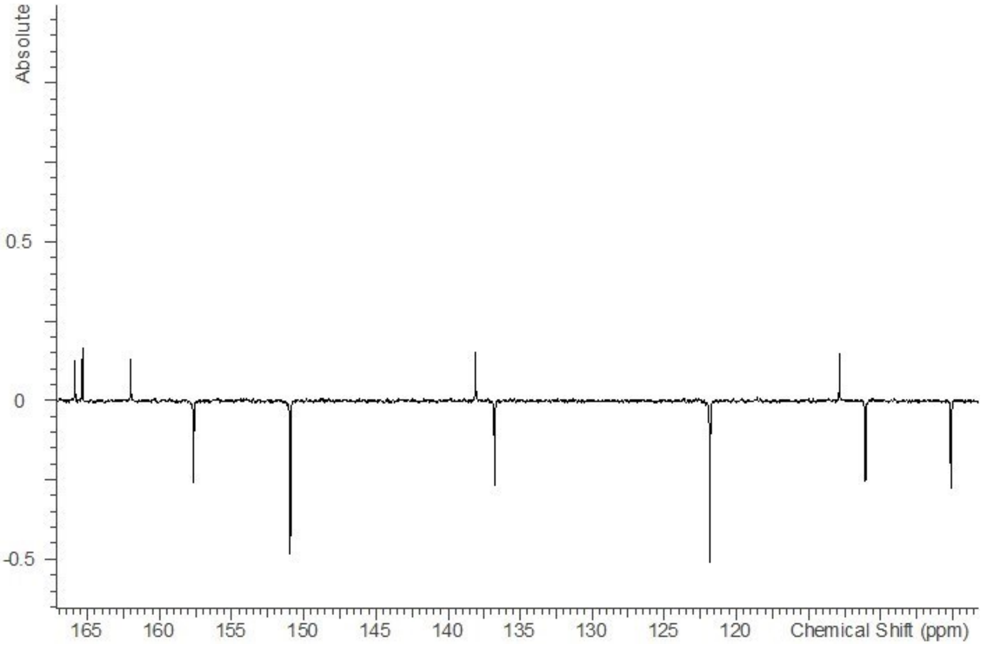

Figure S4 ^{13}C NMR spectra of **2** in dmso-d_6.

Acetamidium octamolybdate salt

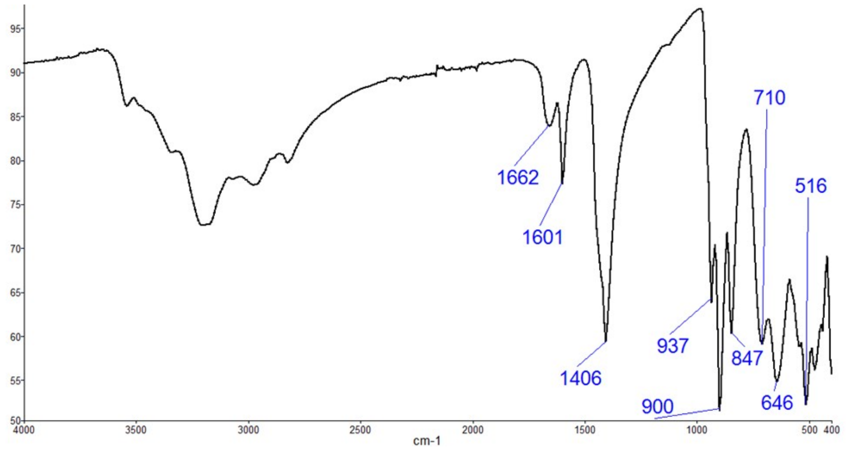

Figure S5. IR spectrum of acetamidium octamolybdate salt.

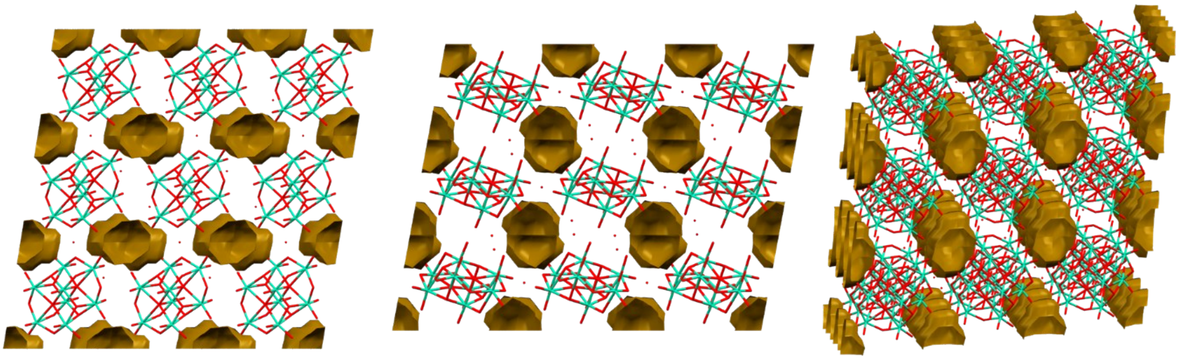

(a) (b) (c)

Figure S6. Tentative crystal structure of acetamidium octamolybdate salt shown parallel to the (a) a-axis, (b) b-axis and (c) in an oblique direction. Crystal structure consists of well defined *β*-octamolybdate anions and four relatively well-defined water molecules, together with well-defined cation accessible voids, which are of the right size for acetamidium ion (void volume 91 Å^3, molecular volume of acetamide from literature[1] 83-86 Å^3). However, electron density maxima in that volume could not be satisfactorily interpreted, partly due to data collection on a severely twinned crystal. Summary of the crystallographic data: a = 7.8083(6) Å, b = 9.7324(7) Å, c = 9.8045(7) Å, α = 97.219(6)°, β = 98.856(7)°, γ = 100.953(6)°, V = 713.51(9) Å^3, R_{int}(hklf5) = 0.052, R_1 = 0.1283, wR_2 = 0.3610, *GooF* = 1.399, completeness = 97%, max/min peak = 4.2/–3.9 e/Å^3.

---

[1] J. W. Bats, M. C. Haberecht, M. Wagner, *Acta Cryst.* **E59** (2003) o1483

X-Ray diffraction - SCXRD

Table S1. BVS calculations for molybdenum atoms in the structures of the prepared hexamolybdate and octamolybdate salts

Hexamolybdates

Compound	Mo1 (complex cation)	Mo2, Mo3, Mo4 (hexamolybdate)
1^{Hw}	6.10	5.99, 5.98, 5.97
2^{Hm}·2MeCN	6.02	5.91, 5.87, 5.95
2^{Hm}·4MeCN	6.29	6.10, 6.05, 6.02
3^{H}	6.22	6.15, 6.05, 6.06
4^{Hw}·4MeCN	6.05	6.00, 5.98, 6.01

Octamolybdates

Compound	Mo1 (complex cation)	Mo2, Mo3, Mo4, Mo5 (octamolybdate)
1^{Ow}·2MeCN·4H_2O	5.95, 6.01	5.93, 5.89, 5.98, 5.89
2^{Ow-2}·4MeCN·2H_2O	6.12	5.95, 5.66, 5.89, 5.94
2^{Ow}·2MeCN·10H_2O	6.02, 6.05	5.82, 5.85, 5.92, 5.70
4^{Ow-2}·2MeCN·3H_2O	6.06	5.94, 5.92, 5.87, 5.72
4^{Ow-2}·3MeCN·4H_2O	6.00	5.87, 5.90, 5.94, 5.73

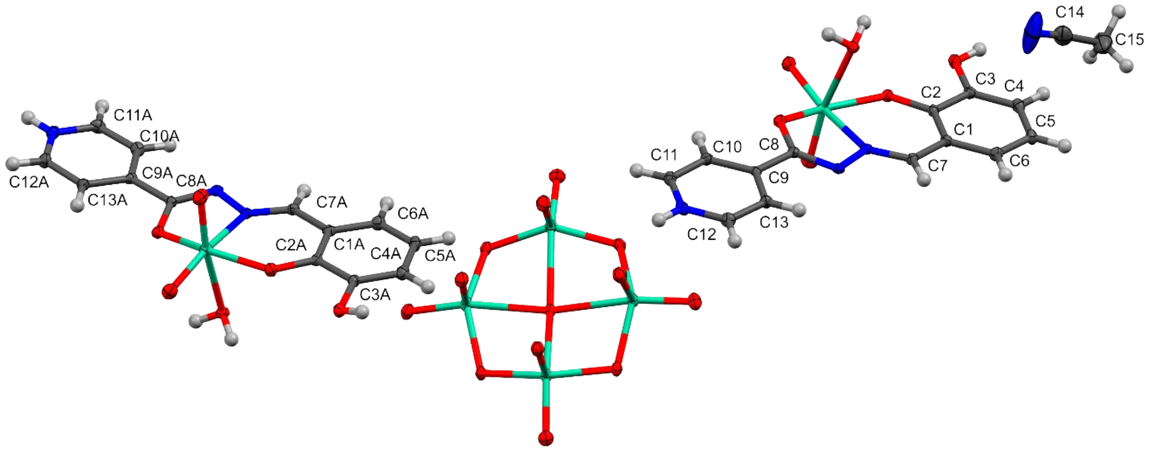
C14
C15
C3
C4
C2
C5
C1
C11
C10
C8
C7
C6
C9
C13
C12
C11A
C10A
C9A
C8A
C12A
C13A
C7A
C6A
C2A
C1A
C4A
C5A
C3A

(a)

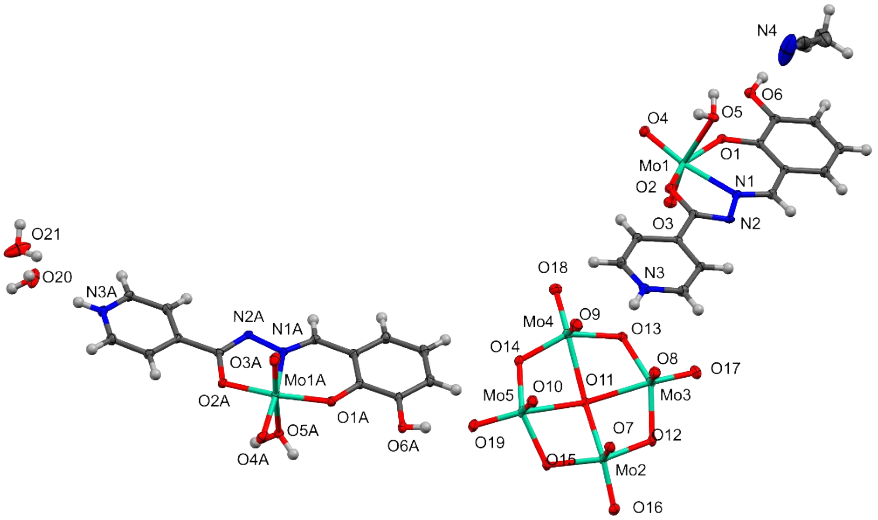
N4
O6
O4
O5
Mo1
O1
N1
O2
N2
O3
O21
O20
N3
O18
N3A
O9
Mo4
O13
N2A
O14
N1A
O8
O17
O3A
O10
O11
Mo5
Mo3
Mo1A
O2A
O1A
O7
O12
O19
O15
O5A
O4A
O6A
Mo2
O16

(a')

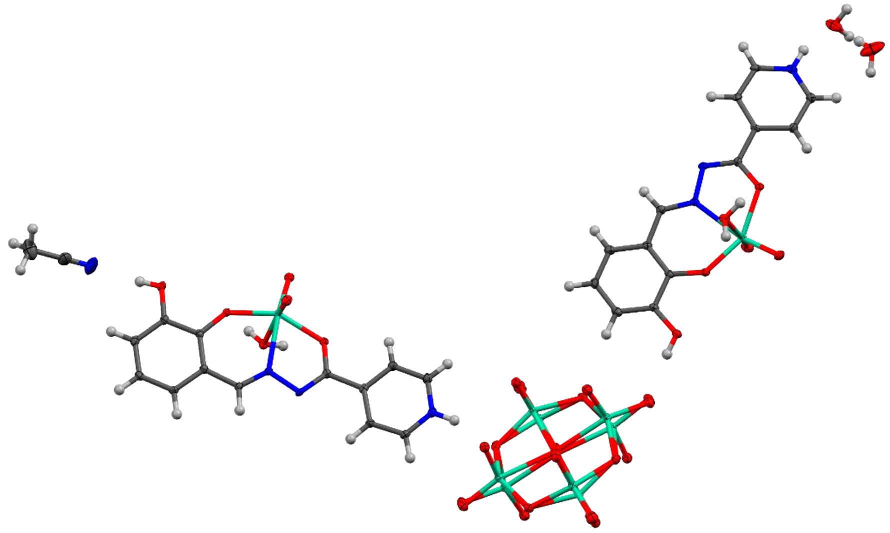

(b)

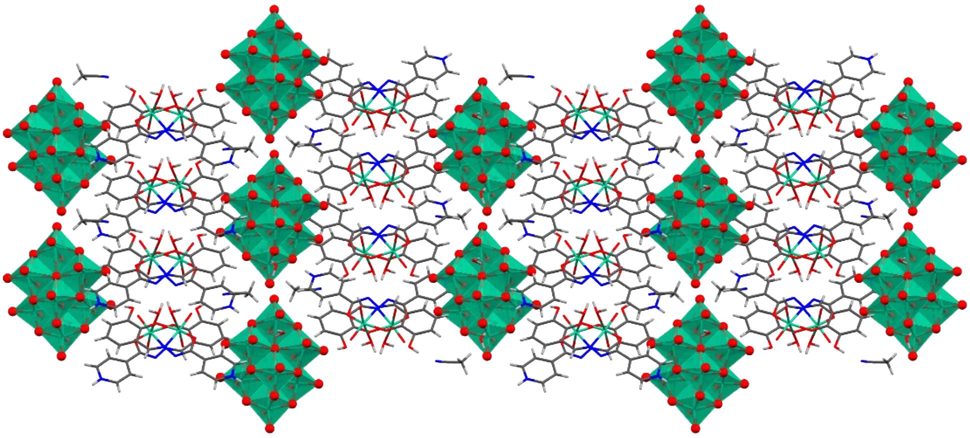

(c)

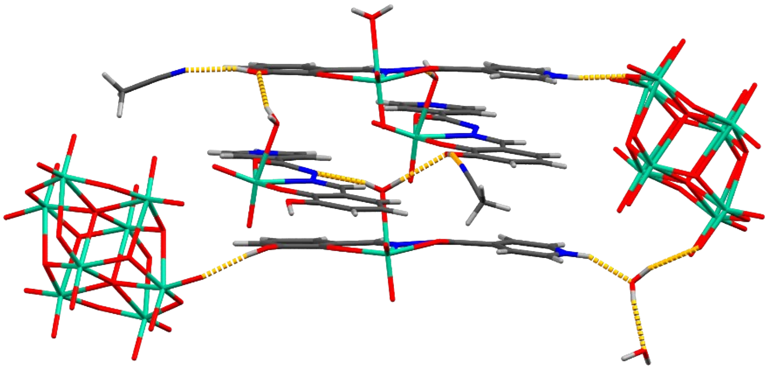

(d)

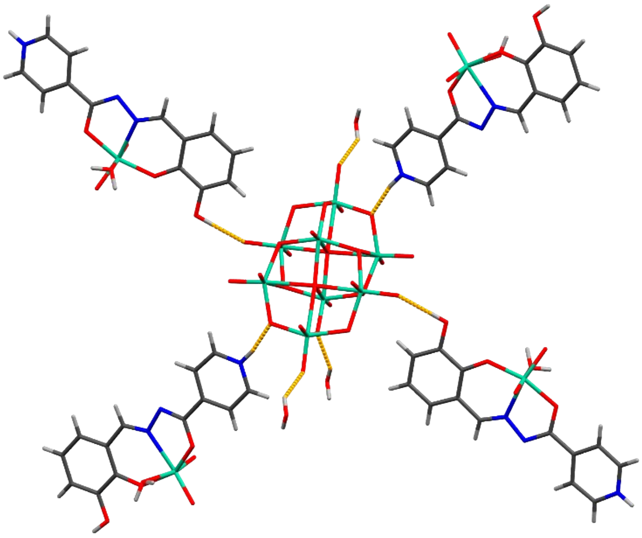

(e)

Figure S7. (a) Carbon atom and (a') non-carbon atom enumeration in the crystal structure of **1**^{Ow}·2MeCN·4H_2O. (b) Molecular structure of the complex salt showing two symmetrically independent complex cations in form of $\{MoO_2(HL)(H_2O)\}^+$, octamolybdate tetraanion, two water molecules and acetonitrile molecule. (c) Crystal packing shown parallel to a-axis. (d) The supramolecular environment of the complex cation. Four cations form a supramolecular tetramer, interacting with (e) anions through the hydroxy group and protonated pyridyl group.

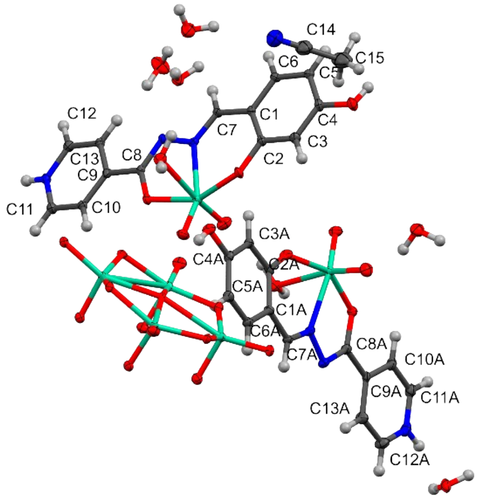
C14
C6
C5
C15
C4
C1
C12
C7
C3
C8
C13
C9
C2
C11
C10
C3A
C4A
C2A
C5A
C1A
C6A
C8A
C7A
C10A
C9A
C11A
C13A
C12A

(a)

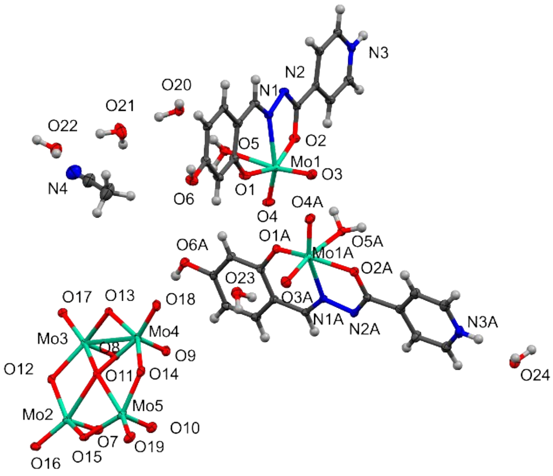
N3
O20
N2
O21
N1
O22
O2
O5
Mo1
N4
O3
O6
O1
O4
O4A
O1A
O5A
O6A
Mo1A
O2A
O23
O17
O13
O18
O3A
N1A
N2A
N3A
Mo3
O8
Mo4
O9
O12
O11
O14
O24
Mo5
Mo2
O10
O7
O19
O16
O15

(a')

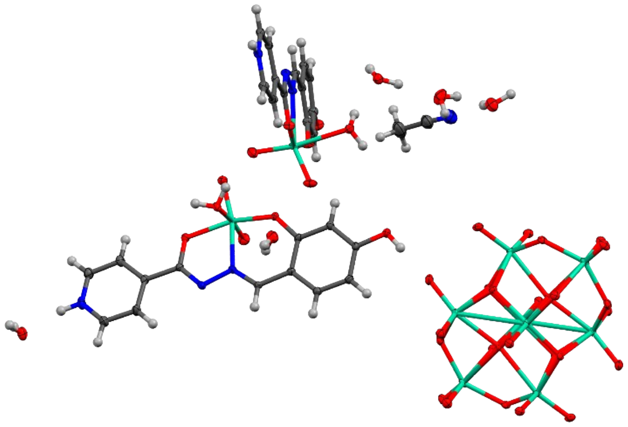

(b)

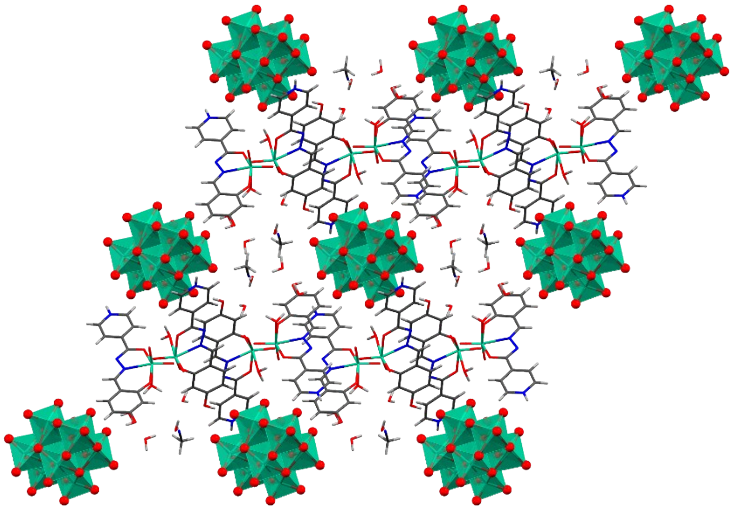

(c)

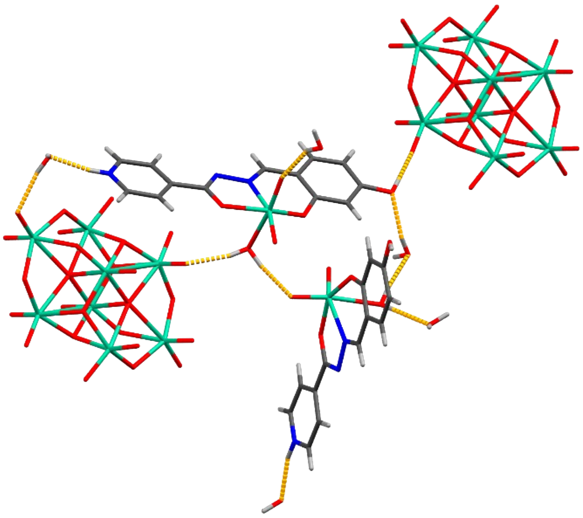

(d)

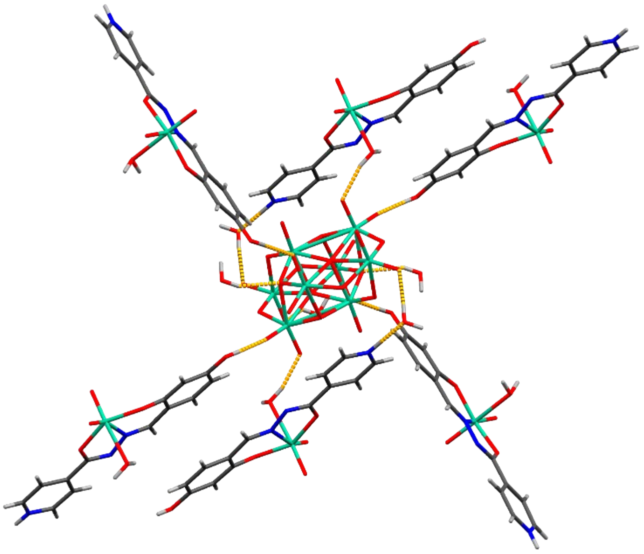

(e)

Figure S8. (a) Carbon atom and (a') non-carbon atom enumeration in the crystal structure of **2**$^{\mathrm{Ow}}$·2MeCN·10H_2O. (b) Molecular structure of the complex salt showing two symmetrically independent complex cations in form of $\{MoO_2(HL)(H_2O)\}^+$, octamolybdate tetraanion, five water molecules and an acetonitrile molecule. (c) Crystal packing shown parallel to a-axis, with solvent-filled canals spanning in the same direction. (d) The supramolecular environment of the complex cation. Two cations are connected through coordinated and solvent water molecules, furthermore interacting with (e) anions through the hydroxy group and the remaining water molecules.

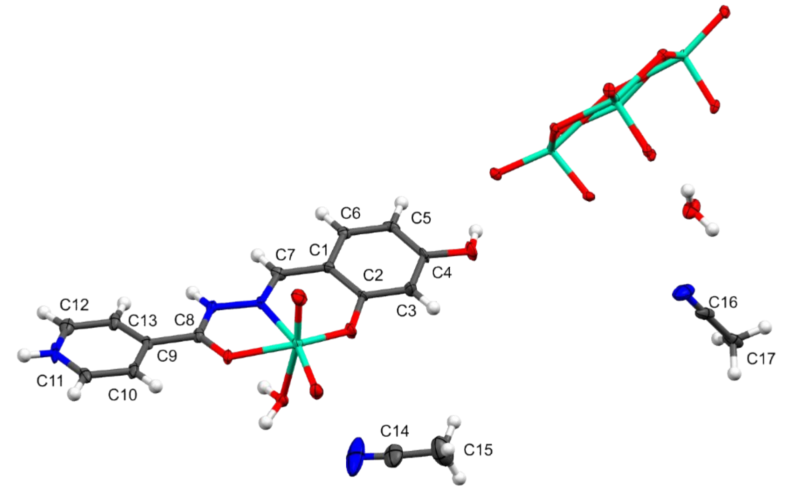
C6
C5
C7
C1
C2
C4
C12
C13
C8
C3
C9
C11
C10
C14
C15
C16
C17

(a)

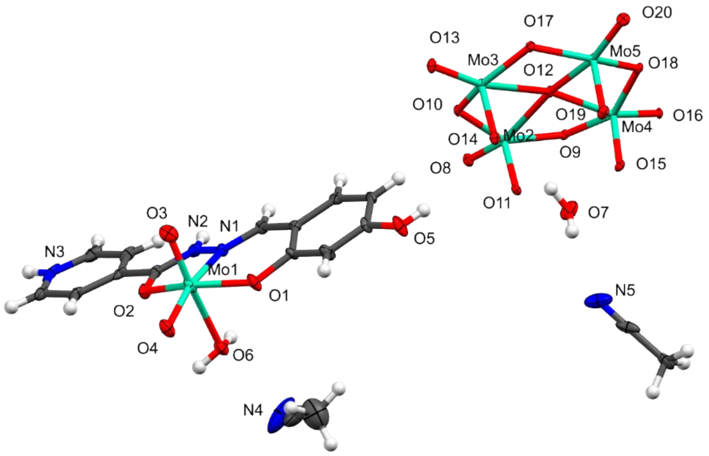
O20
O17
O13
Mo3
Mo5
O18
O12
O10
O19
Mo4
O16
O14
Mo2
O9
O8
O15
O11
O7
O3
N2
N1
N3
Mo1
O5
O2
O1
O4
O6
N5
N4

(a')

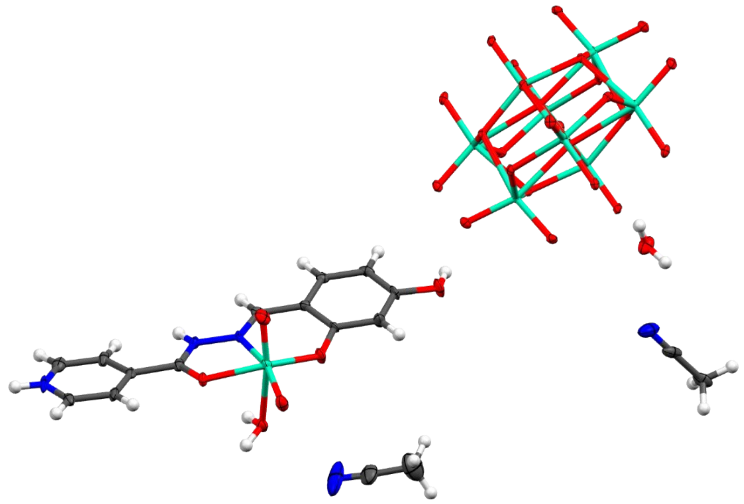

(b)

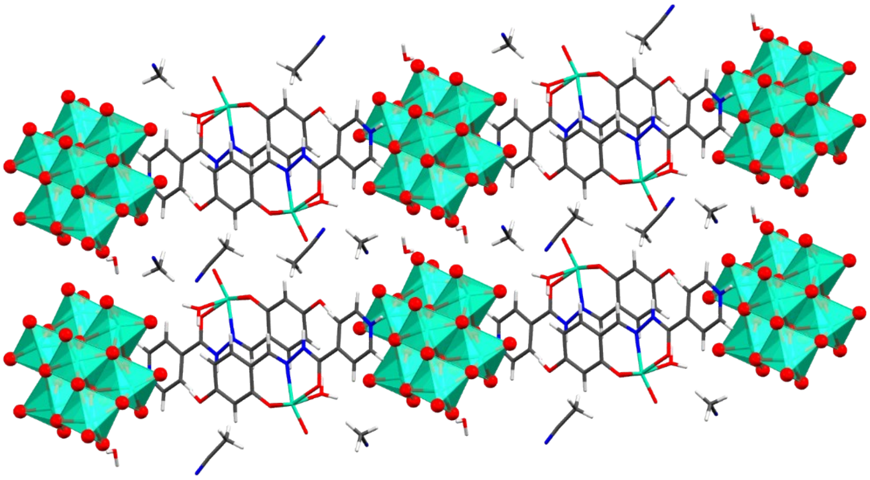

(c)

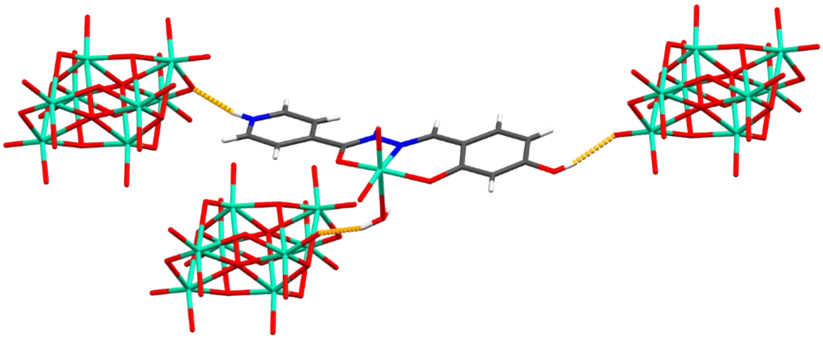

(d)

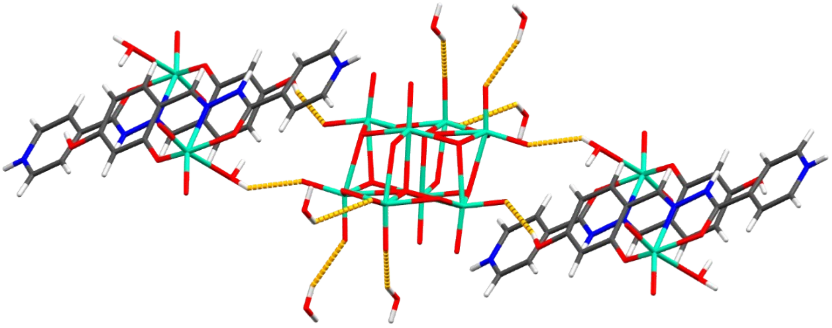

(e)

Figure S9. (a) Carbon atom and (a') non-carbon atom enumeration in the crystal structure of **2**$^{\mathbf{Ow\text{-}2}}$·4MeCN·2H_2O. (b) Molecular structure of the complex salt showing one symmetrically independent complex cation in form of $\{MoO_2(H_2L)(H_2O)\}^{2+}$, octamolybdate tetraanion, one water molecule and two acetonitrile molecules. (c) Crystal packing shown parallel to b-axis, showing solvent-filled layers between the ionic pairs. (d) The supramolecular environment of the complex cation. All available hydrogen bond donors, except for supposedly protonated imino nitrogen, interact with octamolybdate anion (e) whose remaining oxygen atoms interact with the water molecules.

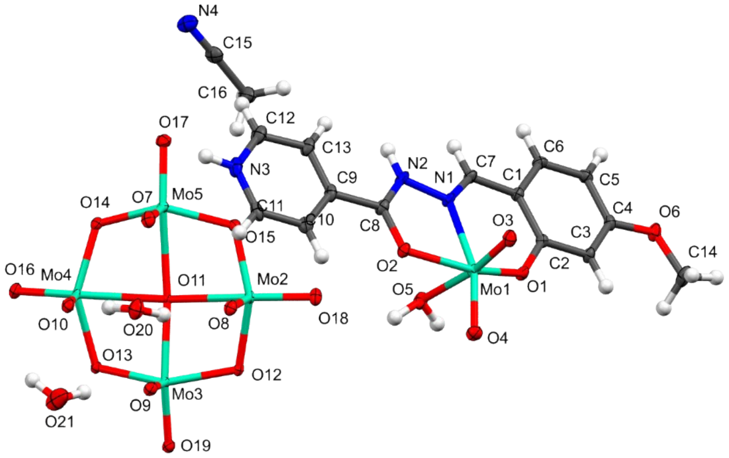
N4
C15
C16
C12
O17
C13
N3
N2
N1
C7
C1
C6
C9
C5
O14
O7
Mo5
C11
C10
C8
O3
C4
O6
C3
O15
O2
C2
C14
O16
Mo4
O11
Mo2
O5
Mo1
O1
O10
O20
O8
O18
O4
O13
O12
O9
Mo3
O21
O19

(a)

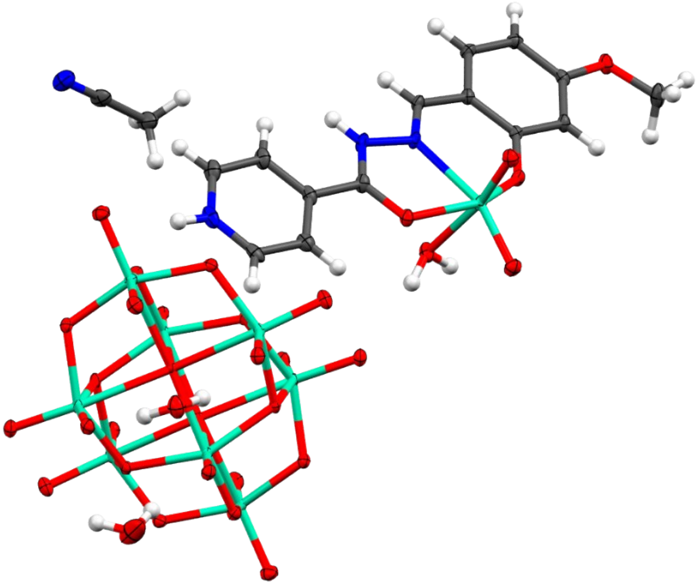

(b)

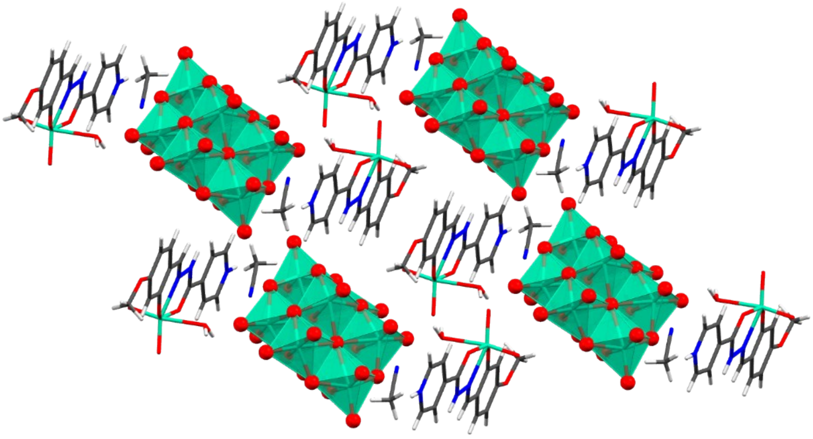

(c)

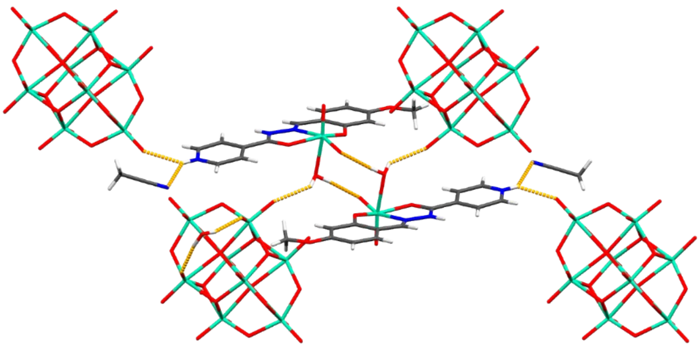

(d)

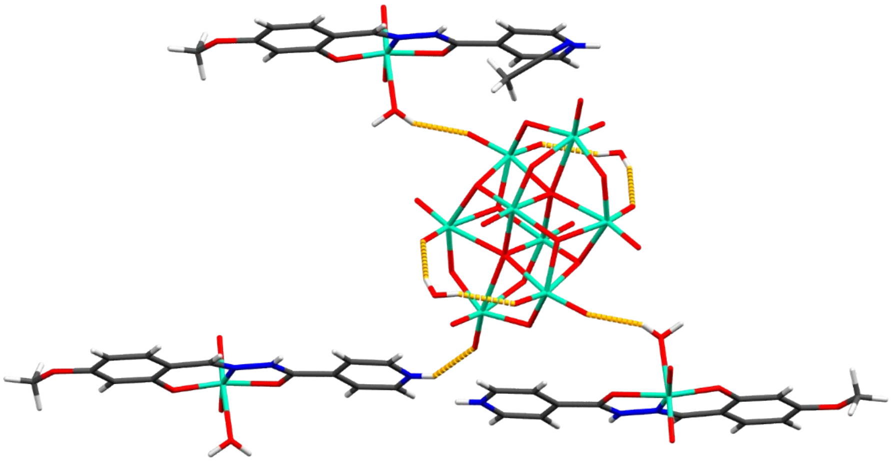

(e)

Figure S10. (a) Atom enumeration in the crystal structure of $\mathbf{4}^{\mathbf{Ow\text{-}2}}\cdot 2MeCN\cdot 3H_2O$. (b) Molecular structure of the complex salt showing one symmetrically independent complex cation in form of $\{MoO_2(H_2L)(H_2O)\}^{2+}$, octamolybdate tetraanion, two water molecules (one ordered and one disordered) and one acetonitrile molecule. (c) Crystal packing shown parallel to a-axis. (d) The supramolecular environment of the complex cation. Cations form a supramolecular dimer that interacts with anions through protonated pyridyl nitrogen atom and a coordinated water molecule. Anion (e) additionally has four terminal oxygen atoms bridged *via* water molecules.

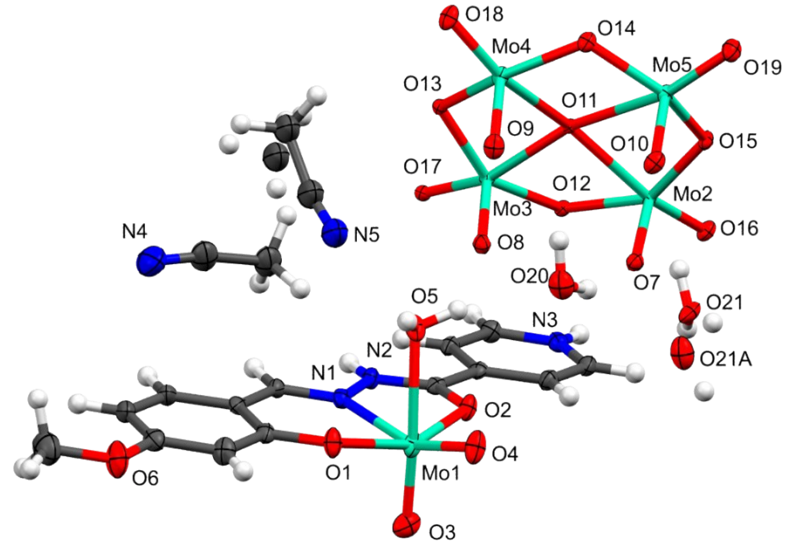
O18
O14
Mo4
Mo5
O19
O13
O11
O9
O10
O15
O17
O12
Mo3
Mo2
O16
N4
N5
O8
O20
O7
O21
O5
N3
N2
N1
O21A
O2
O4
O6
O1
Mo1
O3

(a)

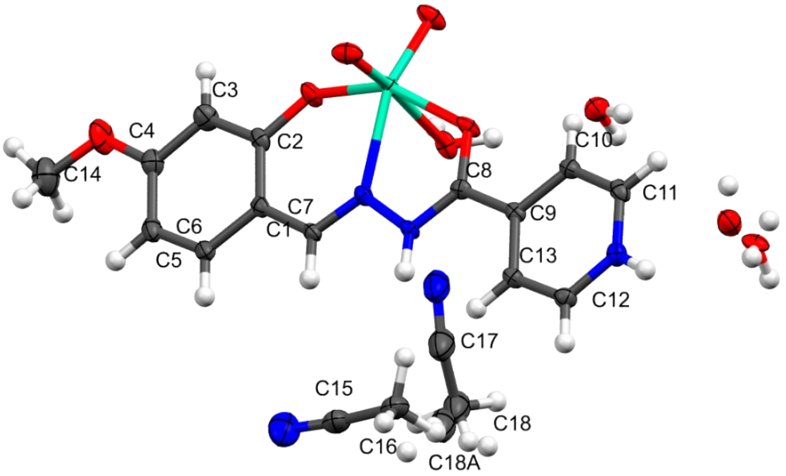
C3
C4
C2
C10
C14
C8
C11
C7
C9
C6
C1
C13
C5
C12
C17
C15
C18
C16
C18A

(a')

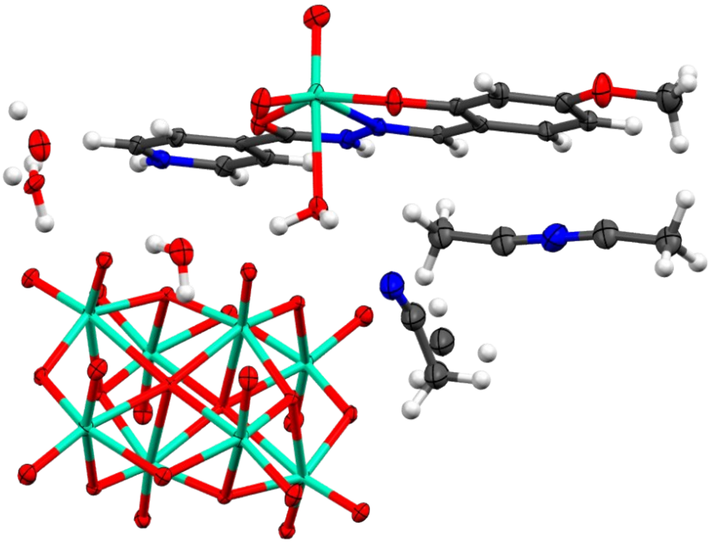

(b)

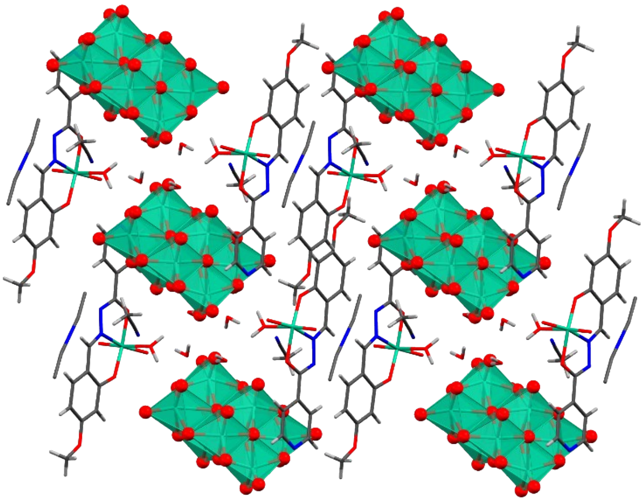

(c)

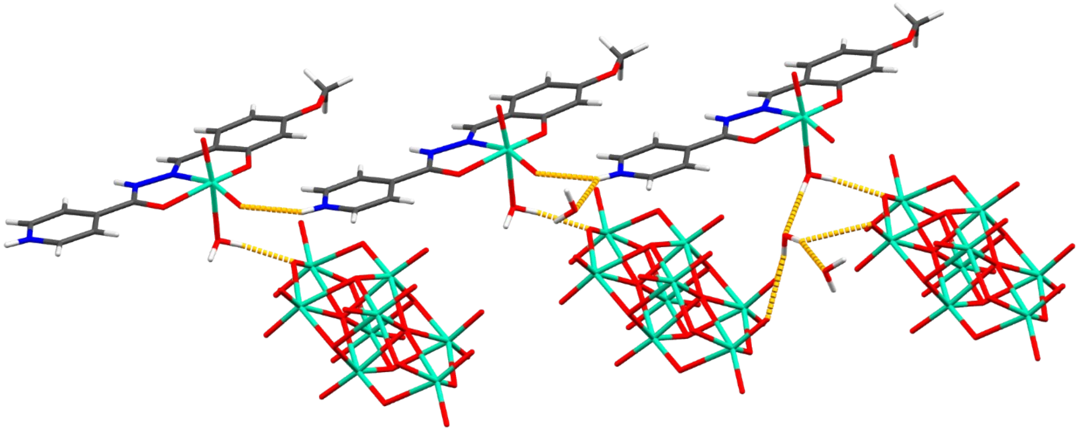

(d)

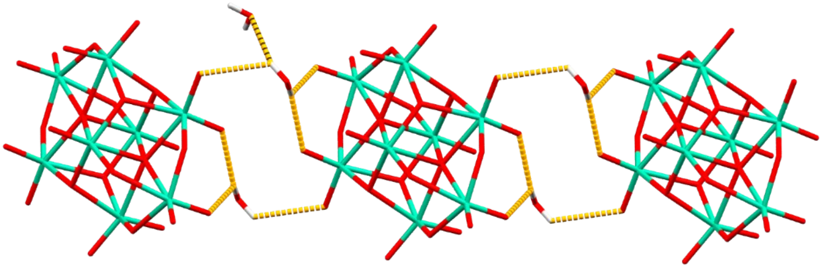

(e)

Figure S11. (a) Heteroatom and (a') carbon atom enumeration in the crystal structure of **$4^{Ow\text{-}2}\cdot 3MeCN\cdot 4H_2O$**. (b) Molecular structure of the complex salt showing one symmetrically independent complex cation in form of $\{MoO_2(H_2L)(H_2O)\}^{2+}$, octamolybdate tetraanion, two water molecules (one of which is disordered on two positions) and two severely disordered acetonitrile molecules, with one of them lying on the symmetry element. (c) Crystal packing shown parallel to a-axis. (d) The supramolecular environment of the complex cation. Cations form a supramolecular chain through $Mo{=}O_e\cdots$pyridinium hydrogen bond which interacts with anions through coordinated water molecules. Anion (e) further interacts with solvent water molecules.

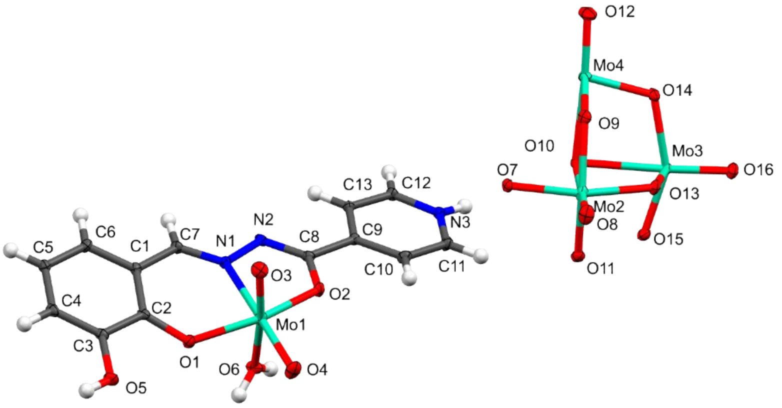
O12
Mo4
O14
O9
O10
Mo3
O16
O7
O13
Mo2
O8
O15
O11
C13
C12
N3
N2
C8
C9
C6
C1
C7
N1
C5
C10
C11
O3
O2
C4
C2
Mo1
C3
O1
O6
O4
O5

(a)

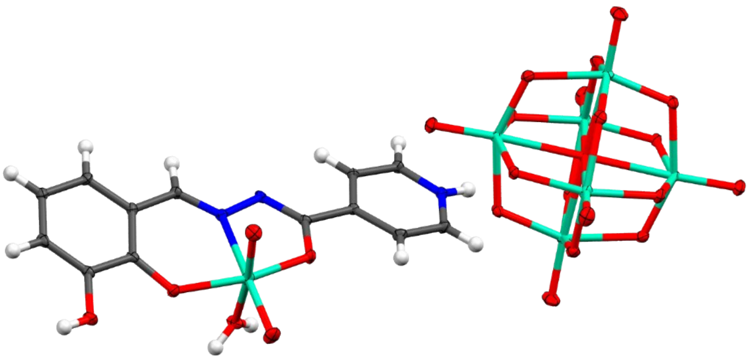

(b)

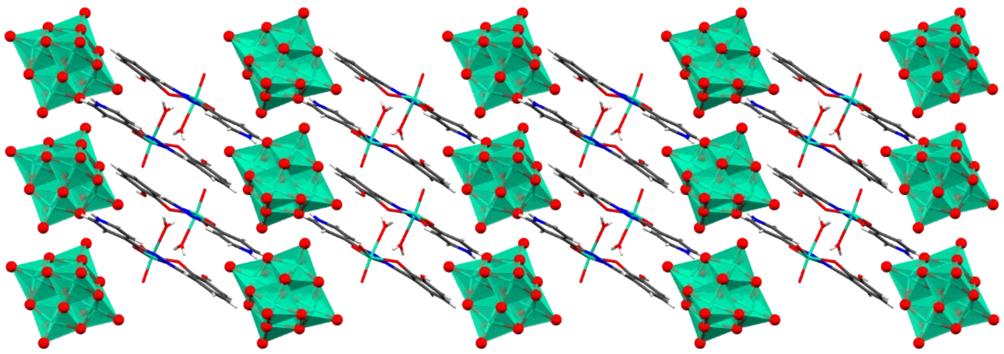

(c)

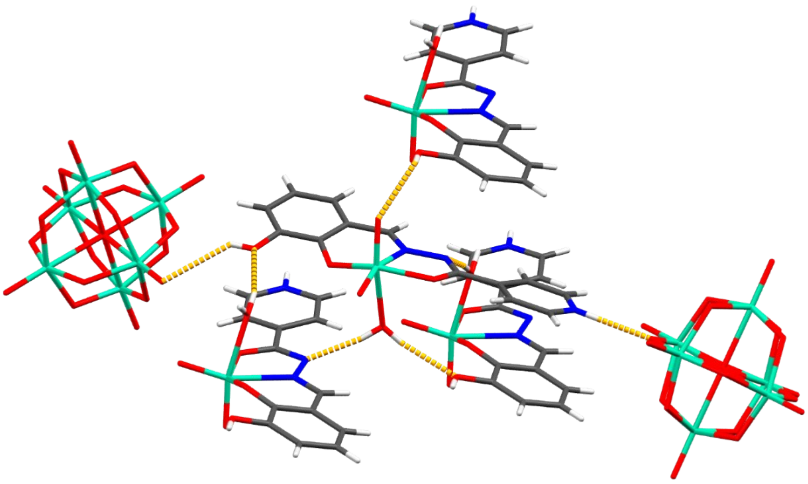

(d)

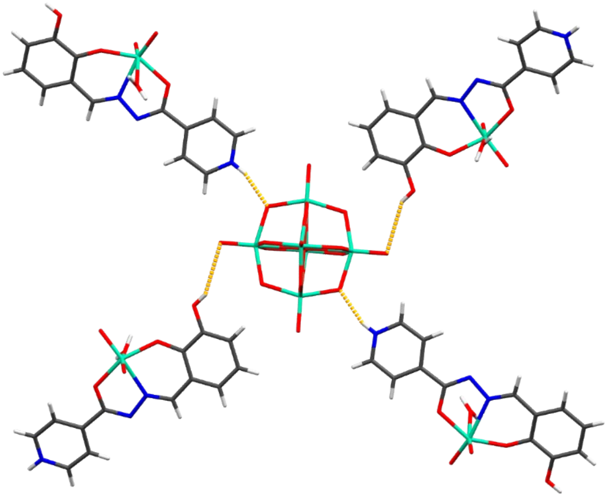

(e)

Figure S12. (a) Atom enumeration in the crystal structure of $\mathbf{1}^{\mathbf{Hw}}$. (b) Molecular structure of the complex salt showing one symmetrically independent complex cation in form of $\{MoO_2(HL)(H_2O)\}^+$ and hexamolybdate dianion. (c) Crystal packing shown parallel to a-axis. (d) The supramolecular environment of the complex cation. Cations form a supramolecular chain through several hydrogen bond interactions between available donors and acceptors, but (e) anion is tightly and symmetrically bound with aryl hydroxy group and pyridinium hydrogen bond donors.

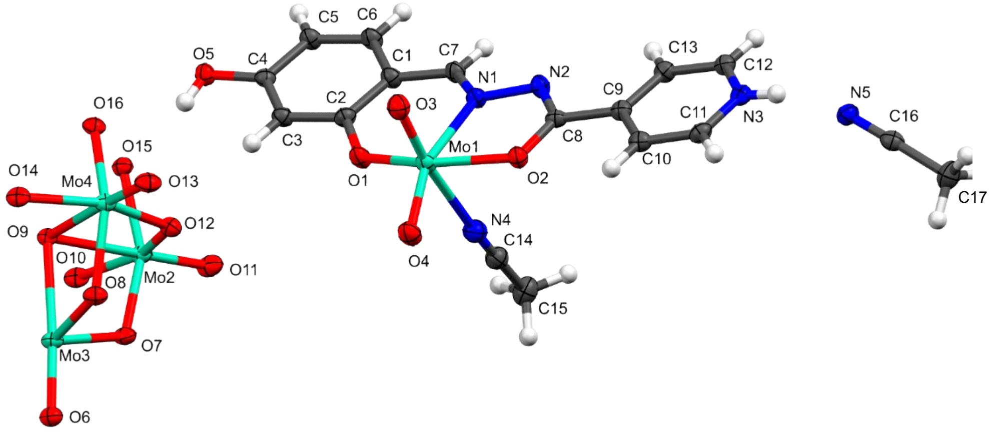
O16
O15
O14
Mo4
O13
O12
O9
O10
O8
Mo2
O11
Mo3
O7
O6
O5
C4
C5
C6
C1
C7
C2
C3
O1
O3
Mo1
N1
N2
C8
O2
O4
N4
C14
C15
C9
C13
C12
C11
N3
C10
N5
C16
C17

(a)

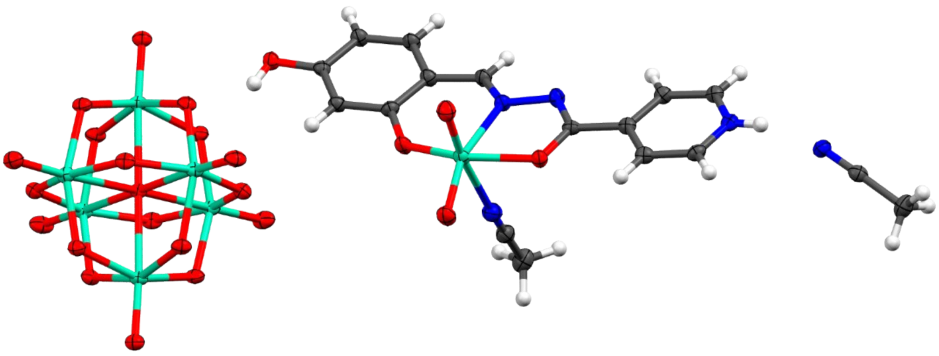

(b)

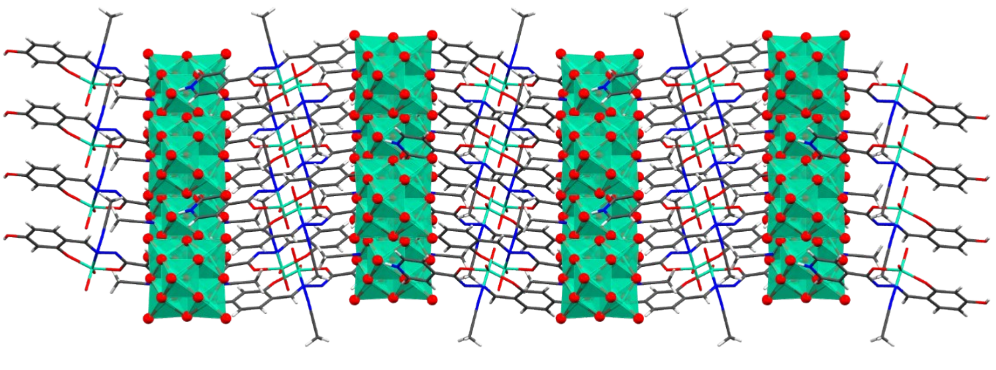

(c)

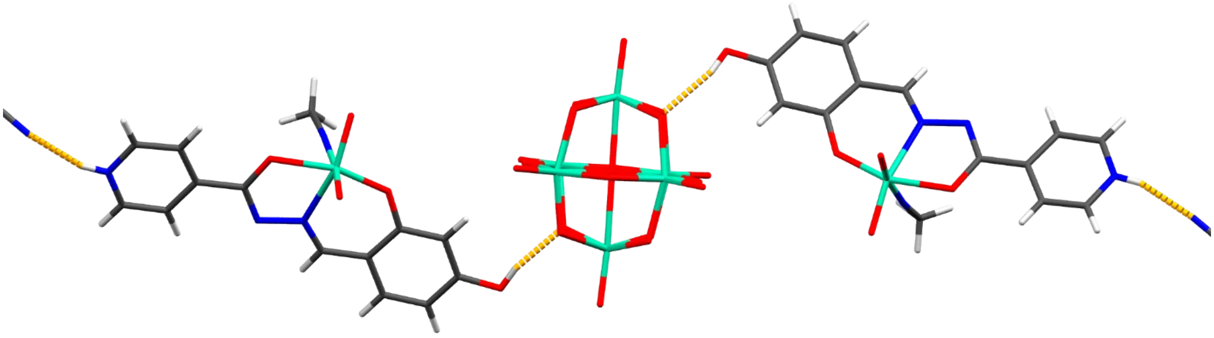

(d)

Figure S13. (a) Atom enumeration in the crystal structure of **2^{Hm}**·2MeCN. (b) Molecular structure of the complex salt showing one symmetrically independent complex cation in form of $\{MoO_2(HL)(MeCN)\}^+$, hexamolybdate dianion and one acetonitrile molecule. (c) Crystal packing shown parallel to b-axis. (d) The supramolecular environment of the complex cation and the anion. Anion is linked to cations through hydrogen bond interaction with the 4-hydroxy group of the ligand, while the pyridinium moiety is linked to the acetonitrile molecule.

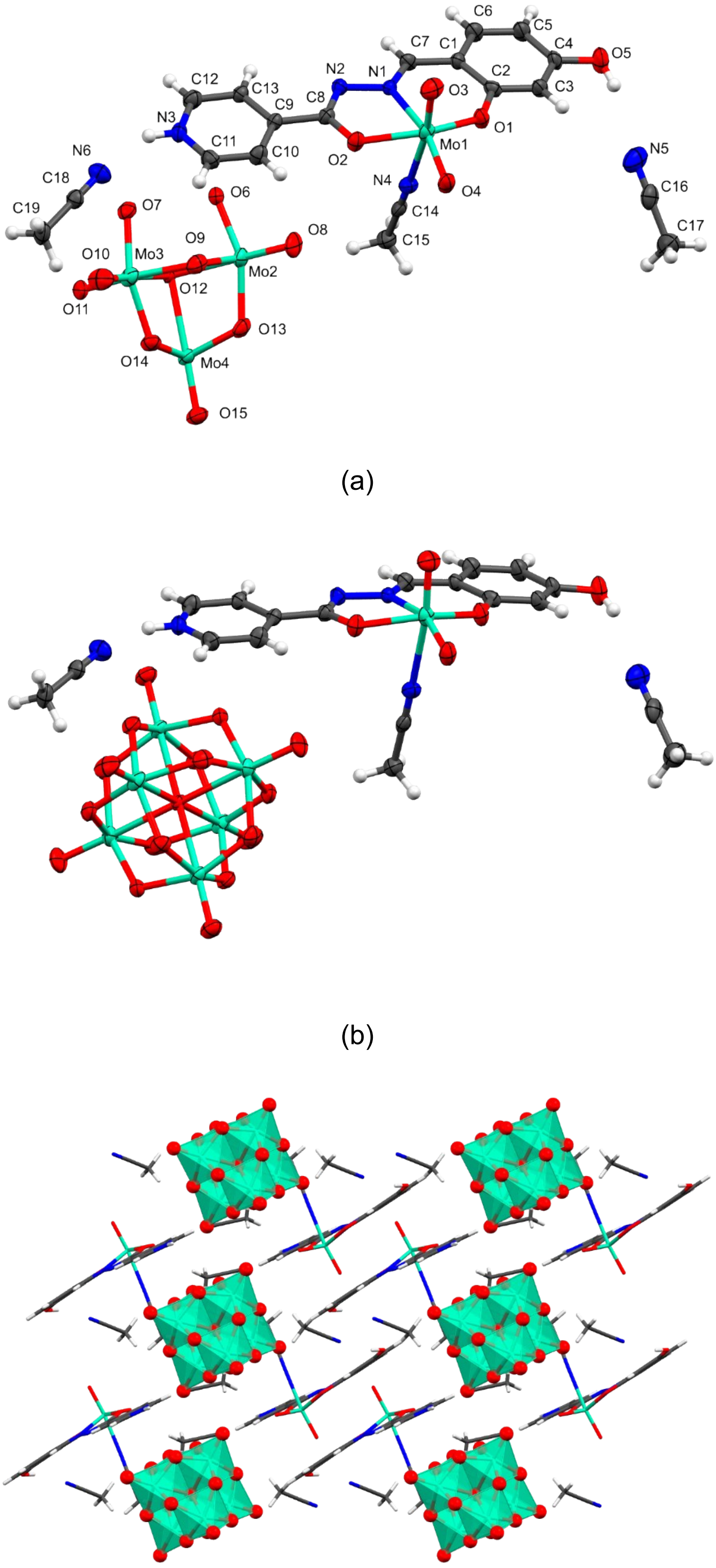
C6
C5
C4
O5
C7
C1
C2
C3
N2
N1
O3
C12
C13
C8
C9
O1
N3
C11
C10
Mo1
N6
O2
N5
C18
N4
O4
C16
C14
O6
C19
O7
O9
O8
C15
C17
O10
Mo3
Mo2
O12
O11
O13
O14
Mo4
O15

(a)

(b)

(c)

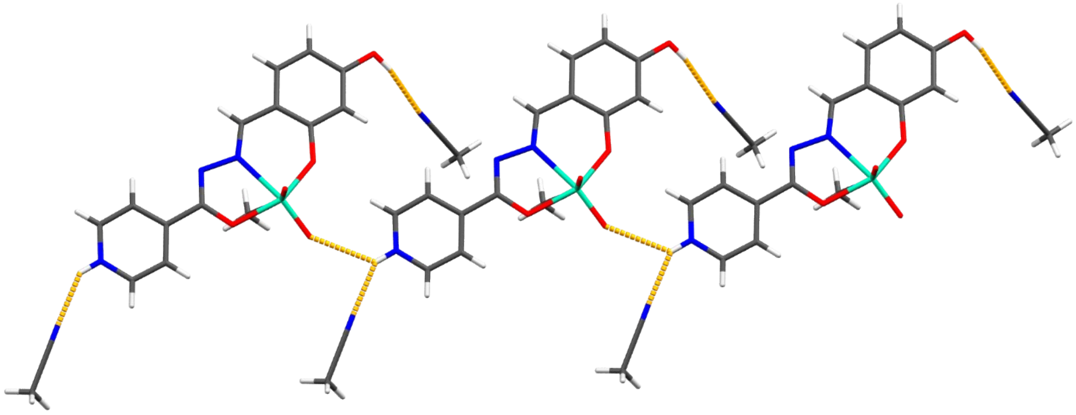

(d)

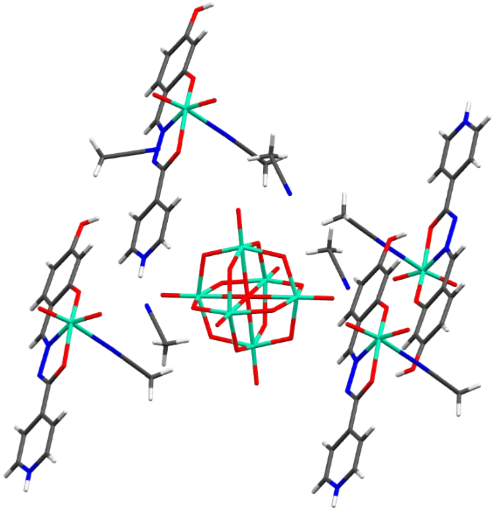

(e)

Figure S14. (a) Atom enumeration in the crystal structure of $\mathbf{2}^{\mathbf{Hm}}\cdot 4MeCN$. (b) Molecular structure of the complex salt showing one symmetrically independent complex cation in form of $\{MoO_2(HL)(MeCN)\}^+$, hexamolybdate dianion and two acetonitrile molecules. (c) Crystal packing shown parallel to a-axis. Solvent-filled voids are situated between the ions. (d) The supramolecular environment of the complex cation. Cations are connected into supramolecular chains through $Mo{=}O_e\cdots$pyridinium hydrogen bond, additionally making interaction with acetonitrile molecules. Surprisingly, anion (e) does not participate in hydrogen bonding, which is in contrast with the structure of $\mathbf{2}^{\mathbf{Hm}}\cdot 2MeCN$**.**

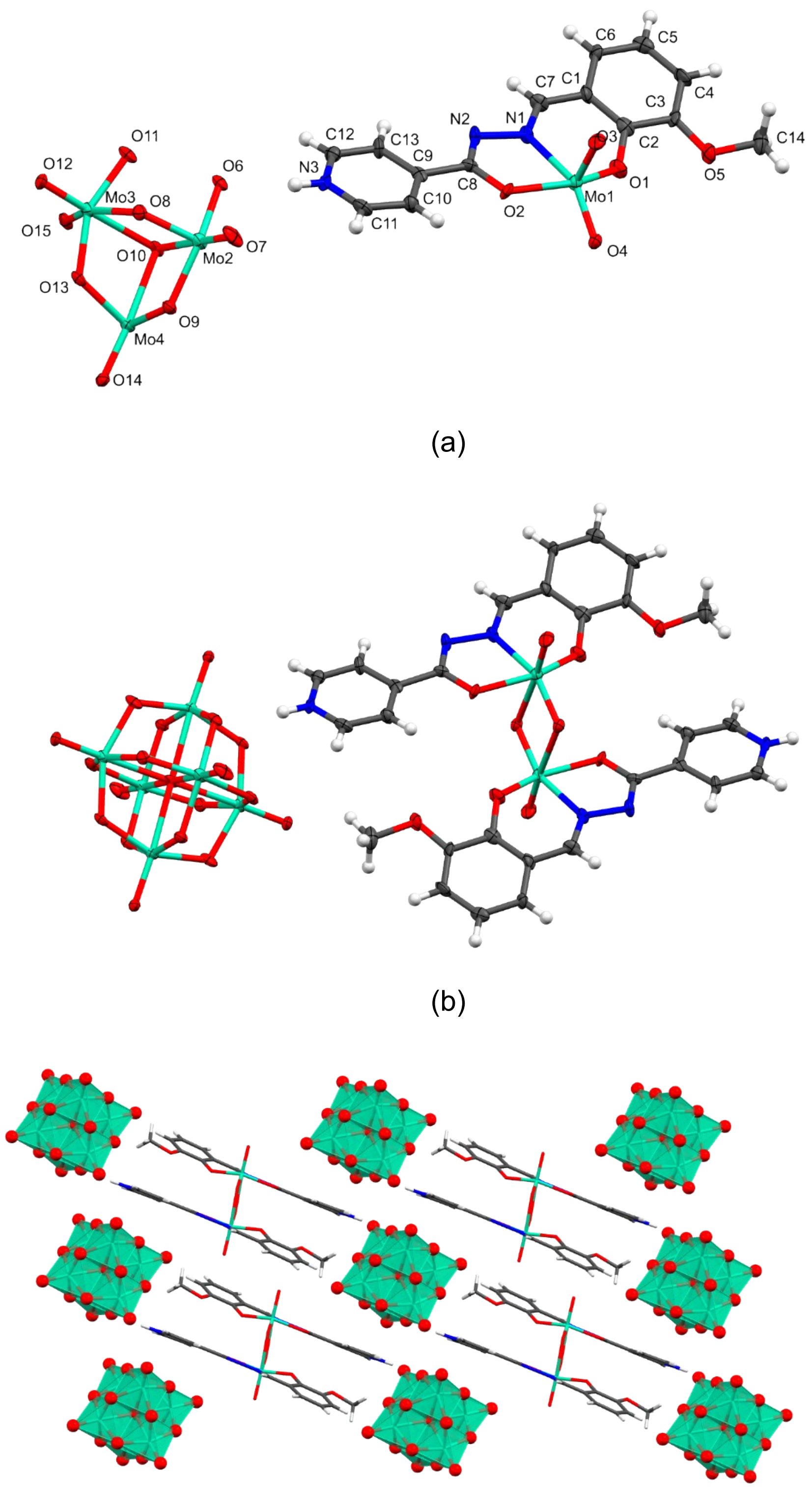
O11
O12
Mo3
O8
O6
O15
O10
Mo2
O7
O13
O9
Mo4
O14
C6
C5
C7
C1
C4
N1
C3
N2
O3
C2
C12
C13
C14
C9
O5
N3
C8
Mo1
O1
C10
O2
C11
O4
(a)
(b)
(c)

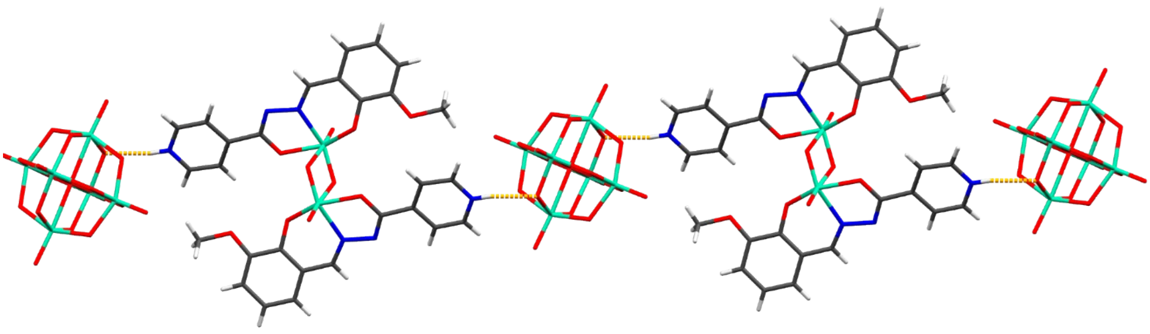

(d)

Figure S15. (a) Atom enumeration in the crystal structure of $\mathbf{3^H}$. (b) Molecular structure of the complex salt showing one symmetrically independent complex dinuclear dication in form of $\{[MoO_2(HL)]_2\}^{2+}$ and hexamolybdate dianion. (c) Crystal packing shown parallel to a-axis. (d) The supramolecular environment of the complex cation. Cations and anions form a remarkably simple supramolecular chain bonded through O_b···pyridinium hydrogen bonds**.**

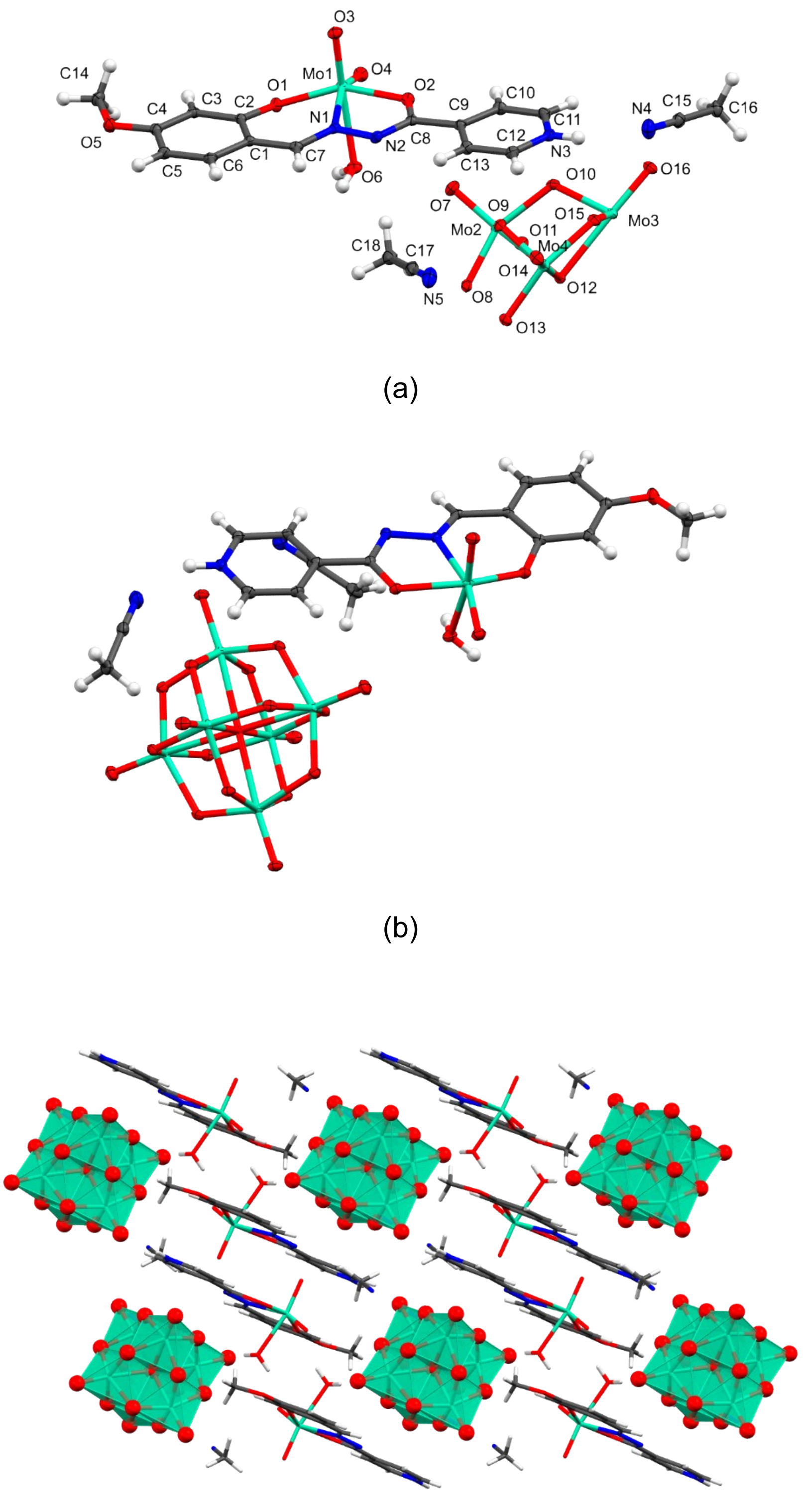
O3
C14
Mo1
O4
O1
O2
C10
C3
C2
C9
N4
C15
C16
C4
N1
C11
O5
C8
N2
C12
N3
C5
C6
C1
C7
C13
O6
O10
O16
O7
O9
O15
Mo3
Mo2
O11
C18
C17
Mo4
O14
O12
N5
O8
O13

(a)

(b)

(c)

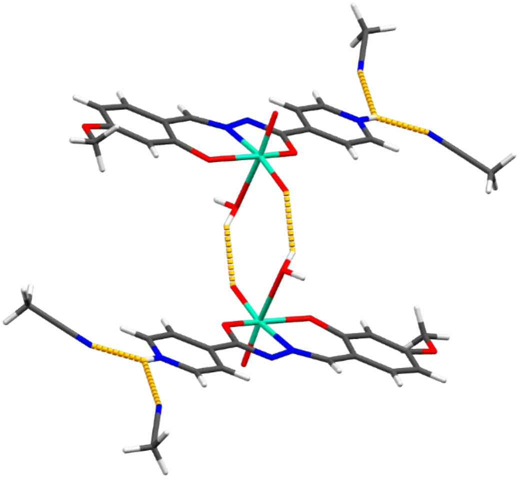

(d)

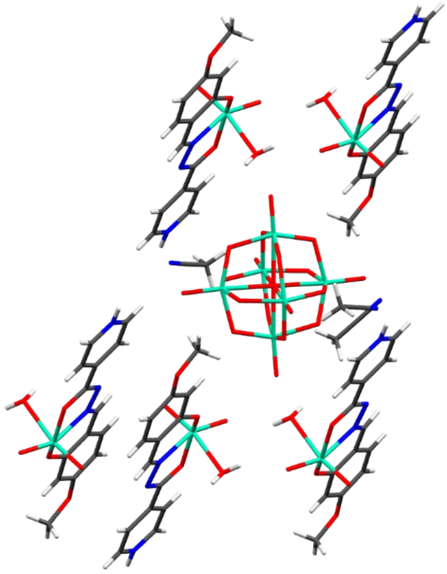

(e)

Figure S16. (a) Atom enumeration in the crystal structure of **4**$^{\mathbf{Hw}}$·4MeCN. (b) Molecular structure of the complex salt showing one symmetrically independent complex cation in form of $\{MoO_2(HL)(H_2O)\}^+$, hexamolybdate dianion and two acetonitrile molecules. (c) Crystal packing shown parallel to a-axis. (d) The supramolecular environment of the complex cation. Cations are connected into supramolecular dimer through $Mo{=}O_e\cdots$coordinated water hydrogen bond, additionally making interaction with all of the acetonitrile molecules *via* pyridinium. Similarly to the structure of **2**$^{\mathbf{Hm}}$·4MeCN, anion (e) does not participate in hydrogen bonding.

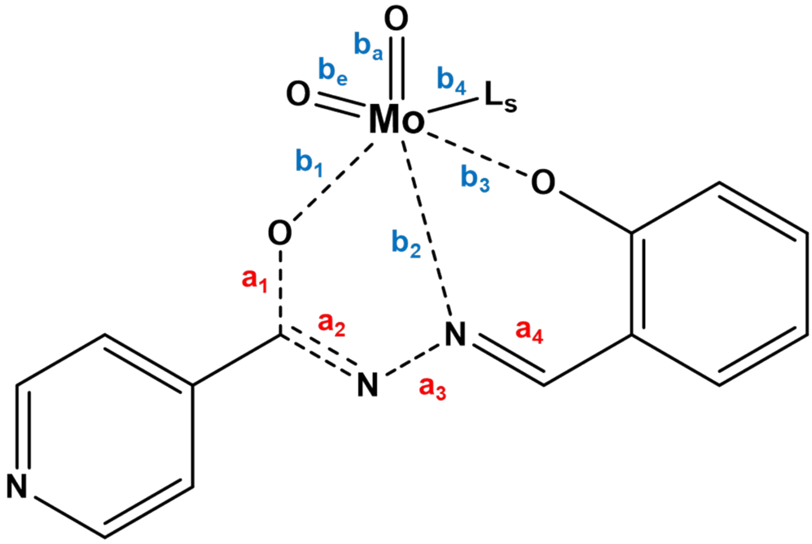

Scheme S2. Bond enumeration for Table S1.

Table S2. Relevant bond lengths (in Å) and interplane angles (in °) for the prepared compounds, with bond enumeration according to Scheme S2. Values lying outside of average±standard deviation are shown in bold type.

Compound	**$1^{Ow}\cdot 2MeCN\cdot 4H_2O$**		**$2^{Ow\text{-}2}\cdot 4MeCN\cdot 2H_2O$**	**$2^{Ow}\cdot 2MeCN\cdot 10H_2O$**		**$4^{Ow\text{-}2}\cdot 2MeCN\cdot 3H_2O$**	**$4^{Ow\text{-}2}\cdot 3MeCN\cdot 4H_2O$**
Hydrazidic C=O (a_1)	1.31	1.31	1.32	1.31	1.32	1.33	1.32
Hydrazide C(=O)-N (a_2)	1.29	1.30	1.29	1.29	1.29	1.29	1.29
Hydrazide N-N (a_3)	1.41	1.41	1.39	1.40	1.40	1.39	1.40
Imine N=C (a_4)	1.28	1.29	1.29	1.29	1.30	1.30	1.30
Mo-hydrazone O (b_1)	2.01	2.00	2.00	2.02	2.01	2.01	2.01
Mo-imine N (b_2)	**2.26**	2.25	2.23	2.24	2.24	2.24	2.23
Mo-aryl O (b_3)	1.93	1.93	1.92	1.92	1.92	1.91	1.93
Mo-solvent O/N (b_4)	2.37	2.36	2.37	2.35	2.35	2.33	2.35
Mo=O axial (b_a)	1.70	1.70	1.70	1.70	1.70	1.69	1.69
Mo=O equatorial (b_e)	1.71	1.71	1.70	1.71	1.70	1.71	1.71
Mo-ONO plane distance	0.33	0.33	0.35	**0.25**	**0.37**	0.33	0.28
Aryl ring interplanar angle	**3.60**	7.70	**12.35**	5.52	9.67	6.18	**3.03**

Compound	**1^{Hw}**	**$2^{Hm}\cdot 2MeCN$**	**$2^{Hm}\cdot 4MeCN$**	**3^{H}**	**$4^{Hw}\cdot 4MeCN$**	**Average±std. dev.**
Hydrazidic C=O (a_1)	1.32	1.32	1.33	1.31	1.32	1.32±0.01
Hydrazide C(=O)-N (a_2)	1.30	1.30	1.28	1.28	1.29	1.29±0
Hydrazide N-N (a_3)	1.40	1.39	1.40	1.41	1.40	1.4±0.01
Imine N=C (a_4)	1.28	1.29	1.29	1.30	1.29	1.29±0.01
Mo-hydrazone O (b_1)	2.00	2.01	2.00	2.01	2.02	2.01±0.01
Mo-imine N (b_2)	**2.26**	2.24	2.24	**2.19**	2.23	2.24±0.01
Mo-aryl O (b_3)	1.92	1.94	1.92	1.89	1.92	1.92±0.01
Mo-solvent O/N (b_4)	2.35	**2.45**	**2.44**	2.41*	2.37	2.35±0.01
Mo=O axial (b_a)	1.69	1.70	**1.67**	**1.66**	1.70	1.7±0
Mo=O equatorial (b_e)	1.70	1.70	**1.69**	**1.73**	1.70	1.71±0.01
Mo-ONO plane distance	**0.38**	**0.25**	0.28	0.30	0.29	0.32±0.04
Aryl ring interplanar angle	**18.00**	8.17	9.26	**18.29**	**2.19**	7±3

Table S3. Hydrogen bond descriptors for the prepared compounds. Enumeration of atoms according to Figures S7-16.

Hexamolybdates

1^{Hw}

D−H···A	Symmetry code	*d*(D−H)	*d*(H···A)	*d*(D···A)	∠(D−H···A)
N3−H3···O7		0.82(5)	1.94(5)	2.739(5)	163(5)
O5−H5···O3	*2−x, −1/2+y, 3/2−z*	0.81(5)	2.38(5)	2.964(5)	129(4)
O6−H6A···O5	*1−x, 1/2+y, 3/2−z*	0.82(5)	2.23(5)	2.996(6)	157(5)
O6−H6B···N2	*1−x, −1/2+y, 3/2−z*	0.82(5)	2.01(5)	2.820(6)	172(6)

$2^{\mathrm{Hm}}\cdot$2MeCN

D−H···A	Symmetry code	*d*(D−H)	*d*(H···A)	*d*(D···A)	∠(D−H···A)
N3−H3···N5		0.86(4)	2.01(5)	2.835(7)	162(9)
O5−H5···O15		0.80(5)	1.92(6)	2.695(5)	163(7)

$2^{\mathrm{Hm}}\cdot$4MeCN

D−H···A	Symmetry code	*d*(D−H)	*d*(H···A)	*d*(D···A)	∠(D−H···A)
N3−H3···O4	*x, 1−y, z*	0.86	2.58	3.201(9)	130
N3−H3···N6		0.86	2.11	2.847(10)	143
O5−H5···N5		0.82	2.17	2.963(11)	162
O5−H5···O3	*1−x, 1−y, −z*	0.82	2.56	3.007(10)	116

3^{H}

D−H···A	Symmetry code	*d*(D−H)	*d*(H···A)	*d*(D···A)	∠(D−H···A)
N3−H3···O14		0.86	2.09	2.973(14)	166

$4^{\mathrm{Hw}}\cdot$4MeCN

D−H···A	Symmetry code	*d*(D−H)	*d*(H···A)	*d*(D···A)	∠(D−H···A)
N3−H3···N4		0.88	2.03	2.790(6)	144
O6−H6A···O7		0.85(4)	1.99(4)	2.830(5)	172(4)
O6−H6A···O4	*1−x, 1−y, 1−z*	0.84(3)	2.18(4)	2.862(4)	138(5)

Octamolybdates

$1^{\mathrm{Ow}}\cdot$2MeCN$\cdot$4H_2O

D−H···A	Symmetry code	*d*(D−H)	*d*(H···A)	*d*(D···A)	∠(D−H···A)
O5A−H5AA···O6	*−x, 1−y, 1−z*	0.87	1.96	2.805(5)	162
O5A−H5AB···N2A	*x, 1/2−y, −1/2+z*	0.87	2.03	2.888(6)	166
N3−H3···O13		0.88	1.82	2.686(6)	169
N3A−H3A···O20		0.88	1.88	2.703(8)	155
N3A−H3A···O10	*−1+x, 1/2−y, 1/2+z*	0.88	2.52	2.947(7)	111
O5−H5B···O6A	*1−x, 1−y, 1−z*	0.87	1.96	2.810(5)	163
O5−H5C···N2	*x, 3/2−y, 1/2+z*	0.87	2.06	2.918(5)	166
O6−H6···N4		0.84	1.9	2.729(13)	168
O6A−H6A···O19		0.84	1.84	2.678(6)	174
O20−H20A···O8	*−1+x, 1/2−y, 1/2+z*	0.87	2.2	3.047(7)	164
O20−H20B···O21		0.87	1.93	2.754(10)	157
O21−H21A···O18		0.87	2.15	2.872(8)	140
O21−H21B···O16	*1−x, −1/2+y,*	0.87	2.08	2.865(8)	150

	1/2−z				

$2^{\mathrm{Ow\text{-}2}}\cdot 4\mathrm{MeCN}\cdot 2\mathrm{H_2O}$

D−H···A	Symmetry code	*d*(D−H)	*d*(H···A)	*d*(D···A)	∠(D−H···A)
N3−H3···O10	*2−x, 1−y, 1−z*	0.88	1.93	2.796(8)	168
O5−H5···O8		0.84	1.91	2.707(7)	158
O6−H6A···N4		0.85(8)	1.98(9)	2.822(13)	169(4)
O6−H6B···O20	*1+x, y, −1+z*	0.86(6)	2.52(13)	2.815(7)	101(9)
O6−H6B···N1	*Intramolecular*	0.86(6)	2.48(12)	2.813(8)	104(10)
O7−H7A···O14		0.85	2.12	2.942(8)	164
O7−H7A···O13	*−x, 2−y, 2−z*	0.85	2.59	2.998(8)	111
O7−H7B···O19	*−1−x, 2−y, 2−z*	0.85	2.27	3.021(8)	148

$2^{\mathrm{Ow}}\cdot 2\mathrm{MeCN}\cdot 10\mathrm{H_2O}$

D−H···A	Symmetry code	*d*(D−H)	*d*(H···A)	*d*(D···A)	∠(D−H···A)
O5A−H5AA···O9	*1−x, 1−y, 1−z*	0.88	1.9	2.729(7)	158
O5A−H5AB···O3		0.88	1.9	2.757(8)	165
N3−H3···O20	*2−x, −y, 1−z*	0.88	1.96	2.813(8)	164
O6A−H6AA···O18		0.84	1.79	2.628(7)	178
N3A−H015···O24		0.88	1.81	2.682(8)	170
O5−H5A···O20		0.87	1.95	2.783(8)	160
O5−H5B···O23	*1+x, y, z*	0.87	1.96	2.801(8)	161
O6−H6···O7	*−1+x, −1+y, z*	0.84	1.94	2.778(7)	175
O20−H20A···O10	*x, −1+y, z*	0.87	2.44	3.015(9)	124
O20−H20B···O21		0.87	1.77	2.626(9)	168
O21−H21A···O22	*2−x, 1−y, 2−z*	0.87	1.98	2.842(11)	172
O21−H21B···O22		0.87	1.98	2.836(9)	169
O22−H22A···O23	*1−x, 1−y, 2−z*	0.87	1.98	2.852(8)	174
O22−H22B···N4		0.87	2.17	2.998(12)	159
O23−H23A···O3A		0.87	1.92	2.702(7)	150
O23−H23B···O6A	*−1+x, y, z*	0.87	2.01	2.853(8)	162
O24−H24A···O12	*−2+x, −1+y, −1+z*	0.87	1.99	2.810(7)	157
O24−H24B···O19	*−1+x, −1+y, −1+z*	0.87	1.95	2.809(8)	170

$4^{\mathrm{Ow\text{-}2}}\cdot 2\mathrm{MeCN}\cdot 3\mathrm{H_2O}$

D−H···A	Symmetry code	*d*(D−H)	*d*(H···A)	*d*(D···A)	∠(D−H···A)
N3−H3···O17	*3−x, 2−y, 1−z*	0.87(5)	2.18(6)	2.902(6)	141(7)
N3−H3···N4	*3−x, 2−y, 1−z*	0.87(5)	2.52(6)	3.137(8)	129(6)
O5−H5A···O18		0.87	2.14	2.761(4)	127
O5−H5B···O4	*1−x, 1−y, −z*	0.87	2.1	2.954(5)	167
O20−H20A···O10		0.87	2.18	3.016(5)	162
O20−H20A···O10	*3−x, 1−y, 1−z*	0.87	2.49	2.951(5)	114
O20−H20B···O8		0.87	2.07(6)	2.878(6)	166(10)
O21−H21A···O10		0.87	2.57	2.998(13)	111
O21−H21A···O7	*3−x, 1−y, 1−z*	0.87	2.39	3.006(13)	128
O21−H21B···O9		0.87	2.00	2.859(12)	169
O21−H21B···O10		0.87	2.59	2.998(13)	110

$4^{Ow\text{-}2}\cdot 3MeCN\cdot 4H_2O$

D−H···A	Symmetry code	*d*(D−H)	*d*(H···A)	*d*(D···A)	∠(D−H···A)
N3−H3···O4	*x, 1+y, z*	0.86(3)	2.30(3)	3.000(6)	139(4)
N3−H3···O21		0.86(3)	2.27(4)	2.932(11)	134(4)
N3−H3···O21A		0.86(3)	2.15(4)	2.799(12)	132(4)
O5−H5A···O14	*1−x, 1−y, 1−z*	0.91	1.88	2.783(5)	169
O5−H5B···O20		0.91	2.12	3.026(6)	171

Table S4. Contact surface voids volume (in %) and solvent accessible voids volume (in %) for prepared compounds, with solvent molecules removed.

Hexamolybdates

Compound	Contact surface voids volume/%	Solvent accesible voids volume/%
1^{Hw}	0.0	0.0
$2^{Hm}\cdot 2MeCN$	6.9	1.0
$2^{Hm}\cdot 4MeCN$	16.4	3.3
3^{H}	0.0	0.0
$4^{Hw}\cdot 4MeCN$	16.8	3.4

Octamolybdates

Compound	Contact surface voids volume/%	Solvent accesible voids volume/%
$1^{Ow}\cdot 2MeCN\cdot 4H_2O$	10.9	2.3
$2^{Ow\text{-}2}\cdot 4MeCN\cdot 2H_2O$	18.1	7.1
$2^{Ow}\cdot 2MeCN\cdot 10H_2O$	21.5	5.6
$4^{Ow\text{-}2}\cdot 2MeCN\cdot 3H_2O$	10.0	1.7
$4^{Ow\text{-}2}\cdot 3MeCN\cdot 4H_2O$	12.1	2.6

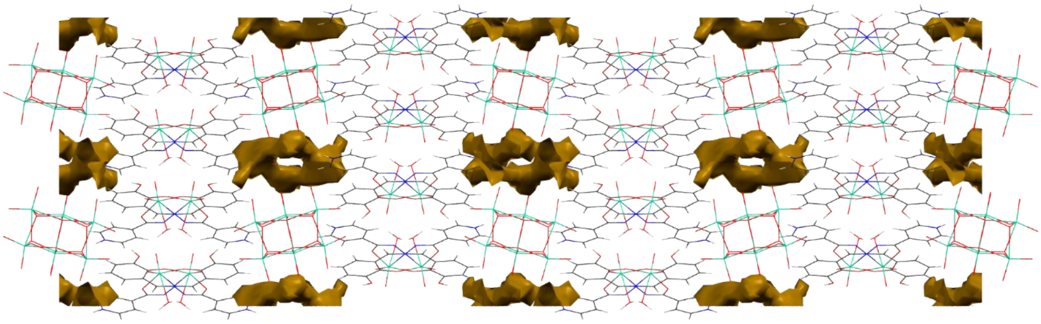

(a)

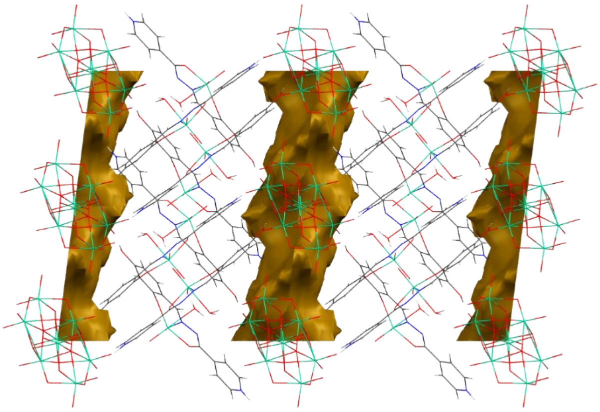

(b)

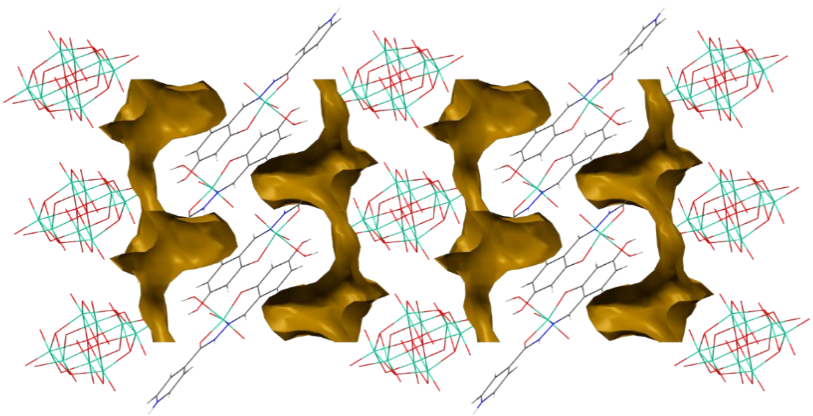

(c)

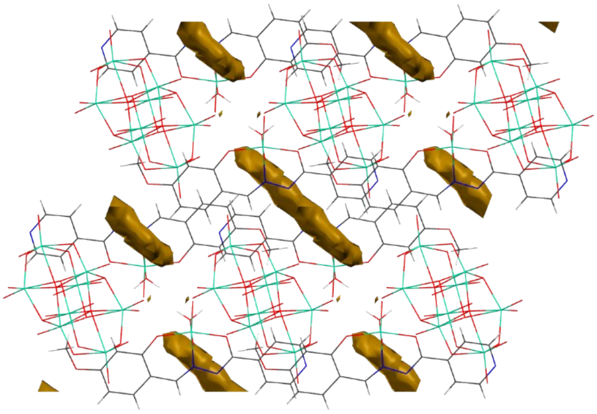

(d)

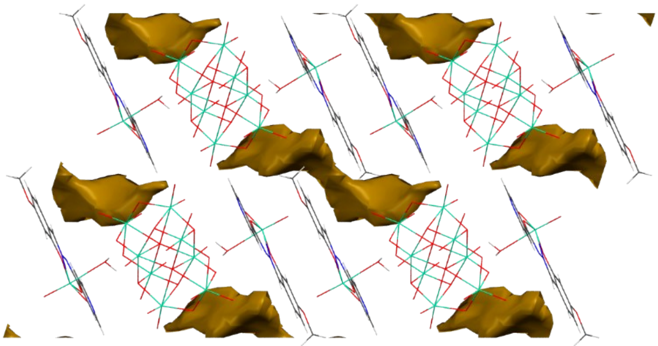

(e)

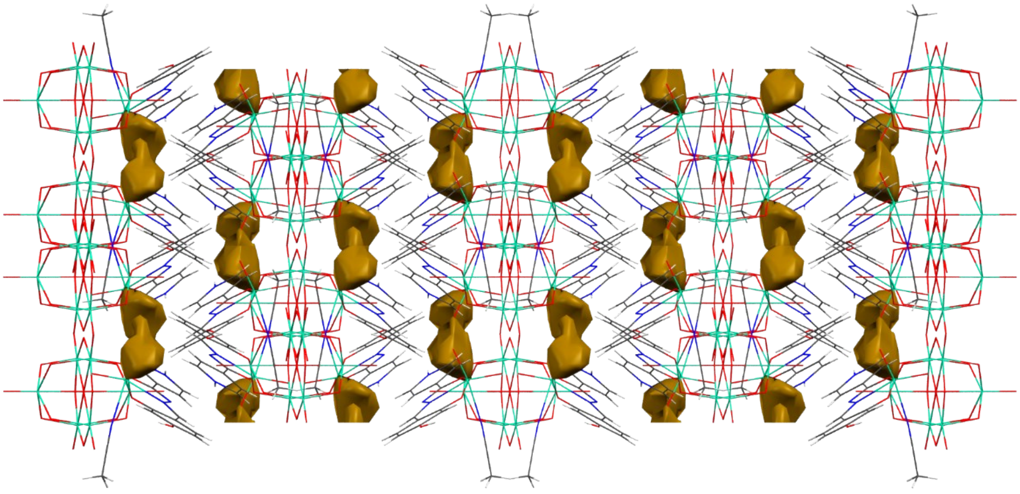

(f)

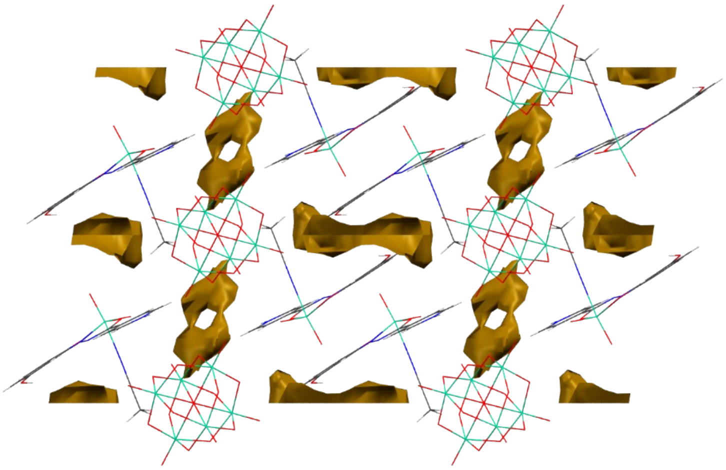

(g)

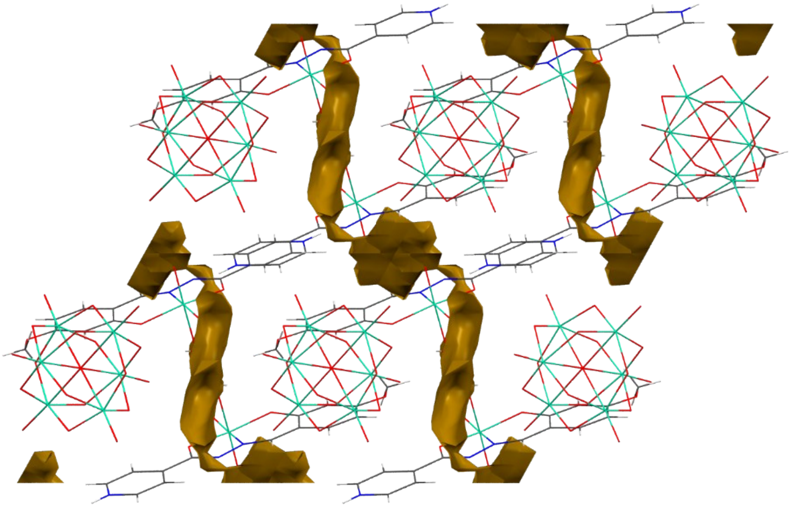

(h)

Figure S17. Solvent accessible voids in the structure of (a) $\mathbf{1}^{\mathbf{Ow}}\cdot2MeCN\cdot4H_2O$, (b) $\mathbf{2}^{\mathbf{Ow}}\cdot2MeCN\cdot10H_2O$, (c) $\mathbf{2}^{\mathbf{Ow\text{-}2}}\cdot4MeCN\cdot2H_2O$, (d) $\mathbf{4}^{\mathbf{Ow\text{-}2}}\cdot2MeCN\cdot3H_2O$**,** (e) $\mathbf{4}^{\mathbf{Ow\text{-}2}}\cdot3MeCN\cdot4H_2O$**,** (f) $\mathbf{2}^{\mathbf{Hm}}\cdot2MeCN$**,** (g) $\mathbf{2}^{\mathbf{Hm}}\cdot4MeCN$**,** (h) $\mathbf{4}^{\mathbf{Hw}}\cdot4MeCN$.

Table S5. General and crystallographic data for prepared octamolybdates

Identification code	**$1^{Ow}\cdot 2MeCN\cdot 4H_2O$**	**$2^{Ow\text{-}2}\cdot 4MeCN\cdot 2H_2O$**	**$2^{Ow}\cdot 2MeCN\cdot 10H_2O$**	**$4^{Ow\text{-}2}\cdot 2MeCN\cdot 3H_2O$**	**$4^{Ow\text{-}2}\cdot 3MeCN\cdot 4H_2O$**
Empirical formula	$C_{56}H_{62}Mo_{12}N_{14}O_{54}$	$C_{34}H_{42}Mo_{10}N_{10}O_{40}$	$C_{56}H_{74}Mo_{12}N_{14}O_{60}$	$C_{32}H_{42}Mo_{10}N_8O_{42}$	$C_{34}H_{47}Mo_{10}N_9O_{42}$
Formula weight	2946.47	2190.17	3054.57	2154.13	2213.21
Temperature/K	170(1)	150(2)	170(1)	170(1)	170(1)
Crystal system	monoclinic	triclinic	triclinic	triclinic	triclinic
Space group	$P2_1/c$	P-1	P-1	P-1	P-1
a/Å	11.0881(2)	7.9678(3)	9.4085(4)	10.5703(2)	10.2611(2)
b/Å	33.6789(5)	10.7556(6)	16.2433(5)	11.3121(2)	10.5249(2)
c/Å	12.0491(2)	18.9607(7)	17.3878(4)	14.2003(2)	15.9967(2)
α/°	90	83.396(4)	116.276(3)	107.1590(10)	100.3730(10)
β/°	108.137(2)	83.567(3)	95.232(3)	102.4120(10)	104.041(2)
γ/°	90	73.581(4)	93.035(3)	105.877(2)	106.410(2)
Volume/Å^3	4275.99(13)	1542.90(12)	2359.80(15)	1477.54(5)	1549.28(6)
Z	2	1	1	1	1
ρ_{calc}g/cm^3	2.288	2.357	2.149	2.421	2.372
μ/mm^{-1}	14.926	2.068	13.601	17.804	17.002
F(000)	2864	1056	1492	1038	1070
Crystal size/mm^3	0.158 × 0.051 × 0.031	0.21 × 0.17 × 0.04	0.34 × 0.19 × 0.04	0.15 × 0.11 × 0.08	0.11 × 0.09 × 0.08
Radiation	CuKα (λ = 1.54184)	MoKα (λ = 0.71073)	CuKα (λ = 1.54184)	CuKα (λ = 1.54184)	CuKα (λ = 1.54184)
2Θ range for data collection/°	8.156 to 160.262	8.078 to 49.998	5.716 to 160.932	6.88 to 160.268	9.09 to 161.488
Index ranges	-13 ≤ h ≤ 14, -42 ≤ k ≤ 39, -14 ≤ l ≤ 15	-9 ≤ h ≤ 9, -12 ≤ k ≤ 12, -21 ≤ l ≤ 22	-12 ≤ h ≤ 11, -19 ≤ k ≤ 20, -22 ≤ l ≤ 19	-13 ≤ h ≤ 13, -14 ≤ k ≤ 13, -18 ≤ l ≤ 18	-13 ≤ h ≤ 12, -13 ≤ k ≤ 13, -20 ≤ l ≤ 19
Reflections collected	37508	11239	37525	40227	44714
Independent reflections	9113 [R_{int} = 0.0567, R_{sigma} = 0.0506]	5423 [R_{int} = 0.0431, R_{sigma} = 0.0669]	10049 [R_{int} = 0.0545, R_{sigma} = 0.0442]	6253 [R_{int} = 0.0529, R_{sigma} = 0.0294]	6624 [R_{int} = 0.0559, R_{sigma} = 0.0301]
Data/restraints/parameters	9113/0/624	5423/0/431	10049/0/655	6253/2/433	6624/27/452
Goodness-of-fit on F^2	1.094	1.072	1.091	1.105	1.087
Final R indexes [I>=2σ (I)]	R_1 = 0.0443, wR_2 = 0.1281	R_1 = 0.0416, wR_2 = 0.0873	R_1 = 0.0515, wR_2 = 0.1458	R_1 = 0.0315, wR_2 = 0.0835	R_1 = 0.0342, wR_2 = 0.0927
Final R indexes [all data]	R_1 = 0.0503, wR_2 = 0.1324	R_1 = 0.0639, wR_2 = 0.1026	R_1 = 0.0535, wR_2 = 0.1479	R_1 = 0.0353, wR_2 = 0.0850	R_1 = 0.0368, wR_2 = 0.0944
Largest diff. peak/hole / e Å^{-3}	1.69/-1.74	1.31/-0.75	2.29/-1.72	0.88/-0.85	1.40/-1.01

Table S6. General and crystallographic data for prepared hexamolybdates

Identification code	**1^{Hw}**	**2^{Hm}·2MeCN**	**2^{Hm}·4MeCN**	**3^{H}**	**4^{Hw}·4MeCN**
Empirical formula	$C_{26}H_{24}Mo_8N_6O_{31}$	$C_{34}H_{32}Mo_8N_{10}O_{29}$	$C_{38}H_{38}Mo_8N_{12}O_{29}$	$C_{28}H_{24}Mo_8N_6O_{29}$	$C_{36}H_{40}Mo_8N_{10}O_{31}$
Formula weight	1684.03	1812.21	1894.32	1676.05	1876.3
Temperature/K	150(2)	170(1)	293(2)	298(2)	150(2)
Crystal system	monoclinic	monoclinic	triclinic	triclinic	triclinic
Space group	$P2_1/c$	C2/c	P-1	P-1	P-1
a/Å	7.6794(2)	21.0479(4)	9.3622(7)	7.5406(6)	10.8617(4)
b/Å	9.3605(3)	8.6686(2)	10.7026(9)	8.6650(15)	10.9074(4)
c/Å	29.2326(9)	29.2039(5)	15.8530(10)	17.325(3)	13.8765(6)
α/°	90	90	106.074(6)	103.429(14)	97.652(3)
β/°	89.706(3)	95.920(2)	92.475(6)	90.359(9)	107.915(3)
γ/°	90	90	107.934(7)	89.999(10)	114.577(4)
Volume/Å^3	2101.30(11)	5300.01(18)	1437.8(2)	1101.0(3)	1356.26(10)
Z	2	4	1	1	1
ρ_{calc}g/cm^3	2.662	2.271	2.188	2.528	2.297
μ/mm^{-1}	2.421	15.881	1.783	2.307	1.891
F(000)	1612	3496	918	802	910
Crystal size/mm^3	0.15 × 0.1 × 0.05	0.207 × 0.149 × 0.074	0.5 × 0.3 × 0.05	0.5 × 0.02 × 0.008	0.21 × 0.13 × 0.11
Radiation	MoKα (λ = 0.71073)	CuKα (λ = 1.54184)	MoKα (λ = 0.71073)	MoKα (λ = 0.71073)	MoKα (λ = 0.71073)
2Θ range for data collection/°	8.052 to 65.474	6.086 to 160.718	8.106 to 65.23	8.006 to 65.446	8.518 to 59.998
Index ranges	-11 ≤ h ≤ 11, -14 ≤ k ≤ 13, -41 ≤ l ≤ 43	-26 ≤ h ≤ 26, -11 ≤ k ≤ 10, -37 ≤ l ≤ 37	-13 ≤ h ≤ 14, -15 ≤ k ≤ 14, -23 ≤ l ≤ 18	-11 ≤ h ≤ 11, -12 ≤ k ≤ 12, -25 ≤ l ≤ 26	-15 ≤ h ≤ 14, -15 ≤ k ≤ 15, -19 ≤ l ≤ 19
Reflections collected	31071	49371	16260	9183	22244
Independent reflections	7112 [R_{int} = 0.0734, R_{sigma} = 0.0725]	5738 [R_{int} = 0.0729, R_{sigma} = 0.0361]	9435 [R_{int} = 0.0653, R_{sigma} = 0.1527]	9183 [Merged R_{int}, R_{sigma} = 0.2860]	7891 [R_{int} = 0.0315, R_{sigma} = 0.0426]
Data/restraints/parameters	7112/4/334	5738/2/376	9435/0/398	9183/0/323	7891/2/395
Goodness-of-fit on F^2	1.089	1.081	0.985	0.780	1.136
Final R indexes [I>=2σ (I)]	R_1 = 0.0525, wR_2 = 0.0952	R_1 = 0.0418, wR_2 = 0.1177	R_1 = 0.0738, wR_2 = 0.1030	R_1 = 0.0765, wR_2 = 0.1486	R_1 = 0.0335, wR_2 = 0.0772
Final R indexes [all data]	R_1 = 0.0827, wR_2 = 0.1056	R_1 = 0.0442, wR_2 = 0.1208	R_1 = 0.1813, wR_2 = 0.1375	R_1 = 0.1783, wR_2 = 0.1747	R_1 = 0.0464, wR_2 = 0.0847
Largest diff. peak/hole / e Å^{-3}	1.89/-0.98	0.89/-1.04	0.88/-0.74	3.61/-1.41	1.44/-0.96

Thermal behaviour

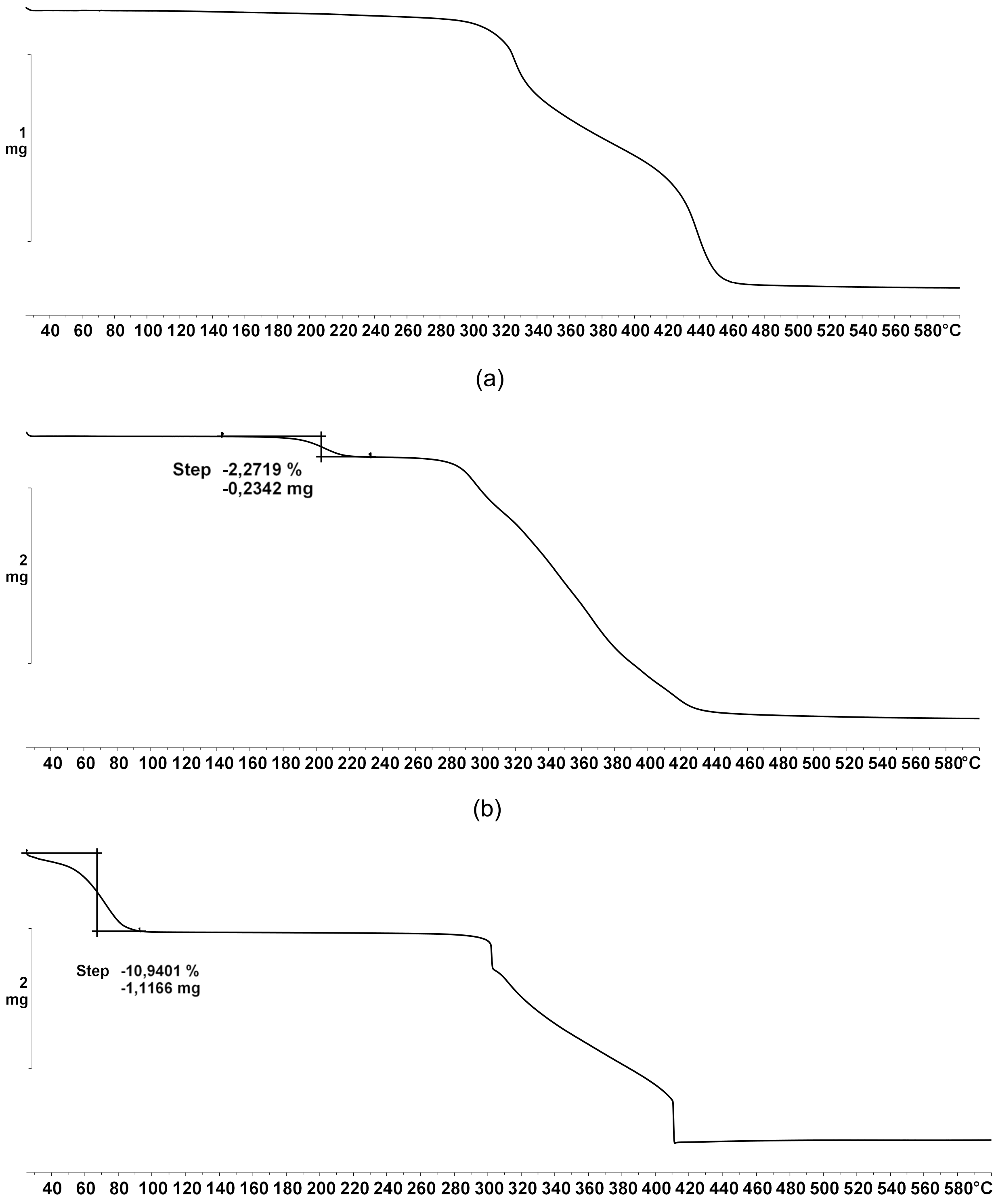

(a)

(b)

(c)

Figure S18. Representative TG curves show weight loss due to (a) decomposition of cation and the cluster in **3**^{H}; (b) loss of coordinated solvent, decomposition of cation and the cluster in **1**^{Hw}; (c) loss of coordinated and lattice solvents, decomposition of cation and the cluster in **4**^{Hw}·4MeCN.

Powder X-ray diffraction patterns – PXRD

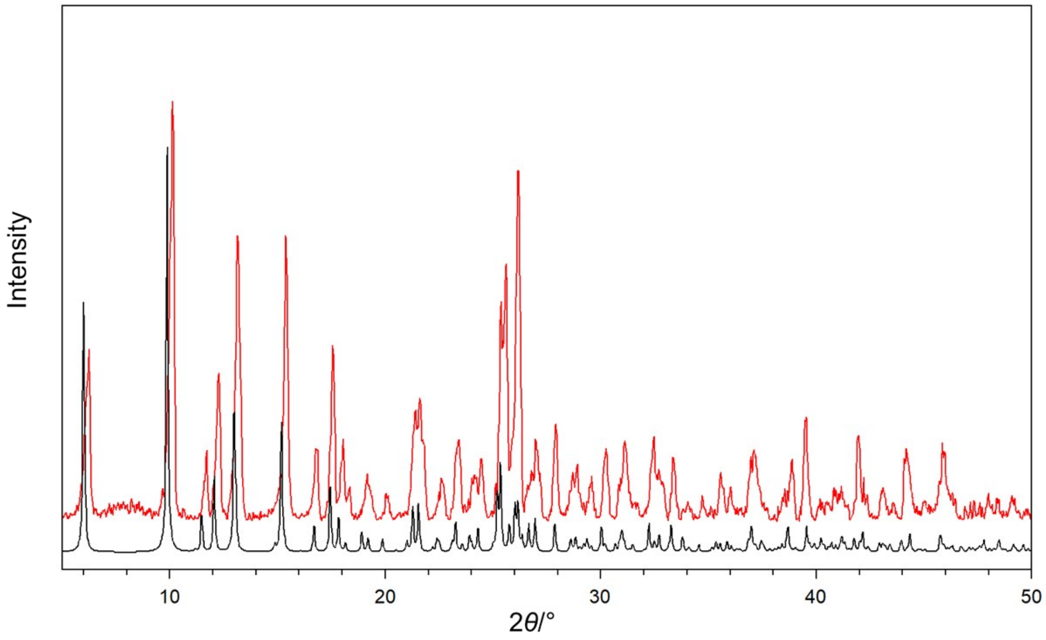

(a)

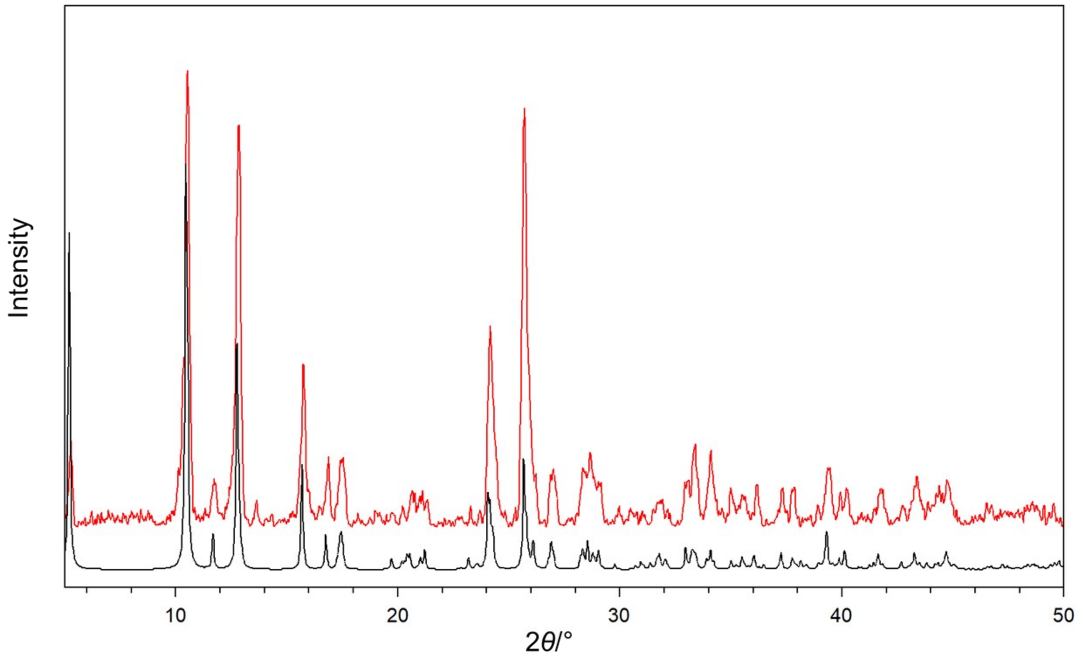

(b)

Figure S19. Powder X-ray diffraction patterns of: (a) **1**$^{\mathbf{Hw}}$ and (b) **3**$^{\mathbf{H}}$. The red lines indicate patterns obtained by powder diffraction, while the black lines indicate patterns calculated from the X-ray single-crystal structures of the corresponding hybrids.

Powder X-ray diffraction patterns of unstable hybrids

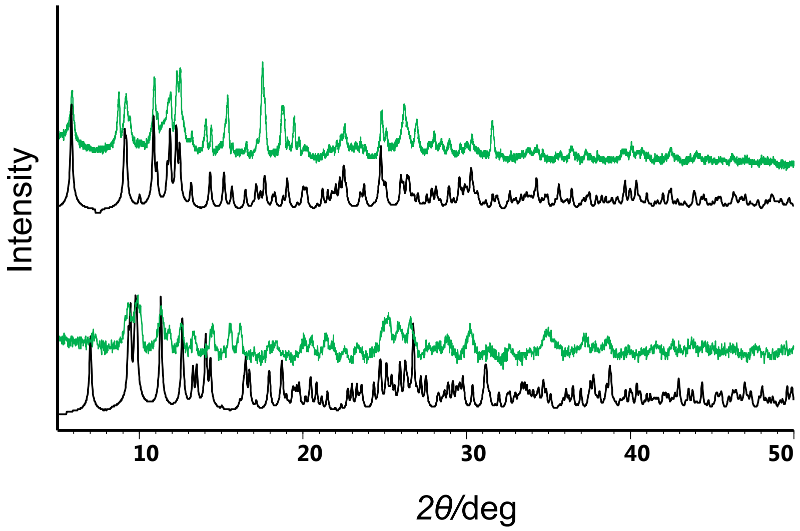

Figure S20. Powder X-ray diffraction patterns of **2**^{Hm}·4MeCN (top) and **4**^{Hw}·4MeCN (bottom). The coloured lines indicate patterns obtained by powder diffraction, CuK_α radiation, while the black lines indicate patterns calculated from the X-ray single-crystal structures of the corresponding compounds.

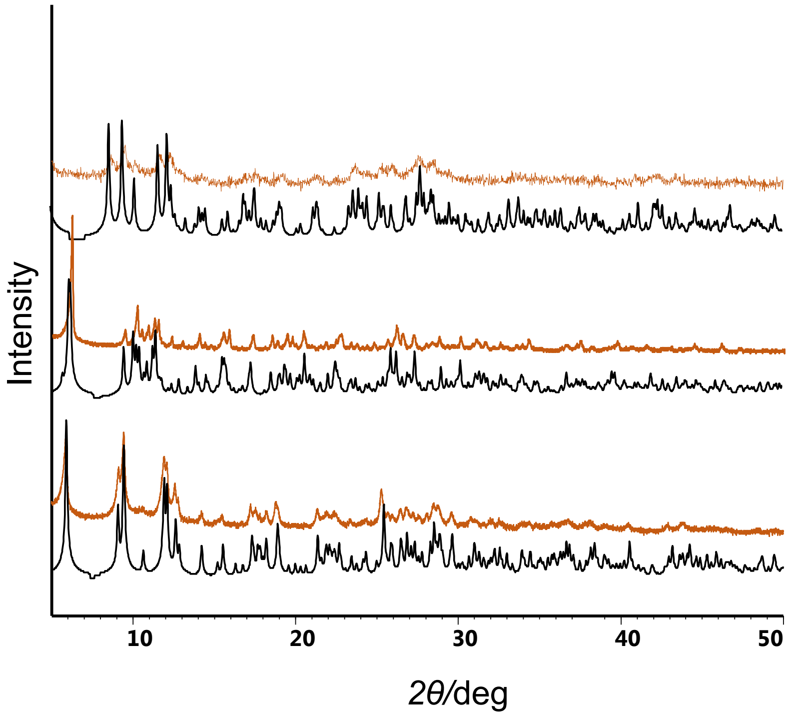

Figure S21. Powder X-ray diffraction patterns of **2**$^{Ow\text{-}2}$·4MeCN·2H_2O, **2**^{Ow}·2MeCN ·10H_2O, and **4**$^{Ow\text{-}2}$·3MeCN·4H_2O (from top to bottom). The coloured lines indicate patterns obtained by powder diffraction, CuK_α radiation, while the black lines indicate patterns calculated from the X-ray single-crystal structures of the corresponding compounds.

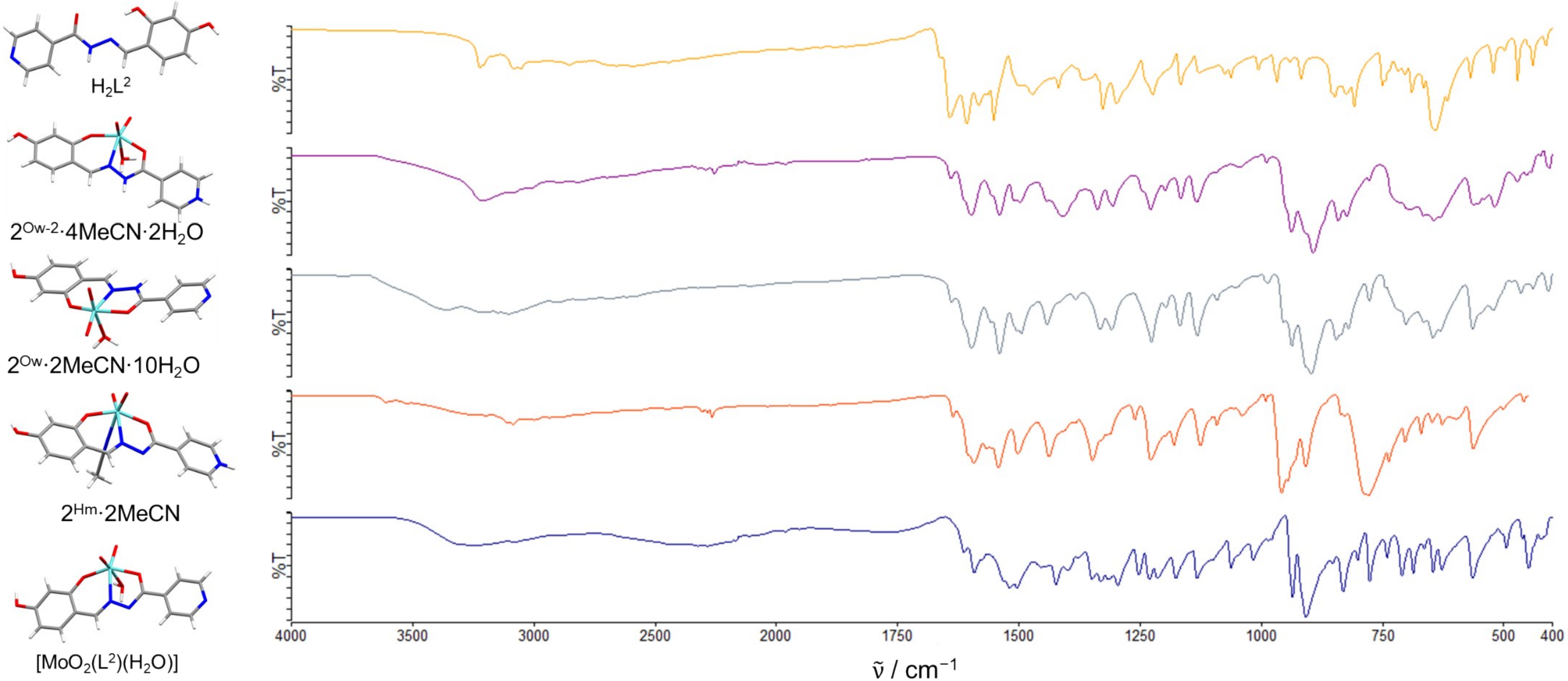

Figure S22. Comparison of IR-ATR spectra of products formed with H_2L^2. Molybdenum complexes of the corresponding compounds and the ligand are depicted on the left side.

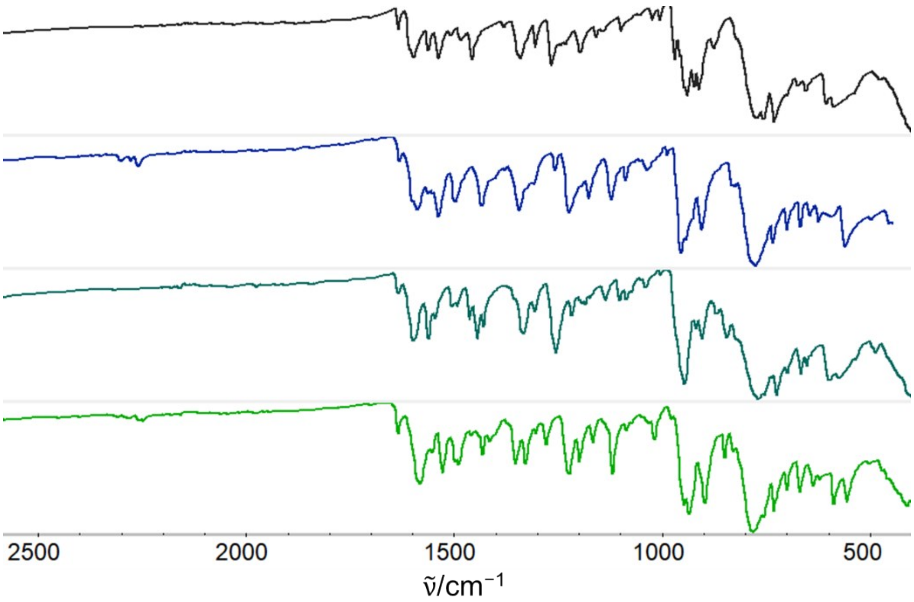

Figure S23. Comparison of IR-ATR spectra of **1**$^{\mathbf{Hw}}$, **2**$^{\mathbf{Hm}}$·2MeCN, **3**$^{\mathbf{H}}$ and **4**$^{\mathbf{Hw}}$**·**4MeCN (from top to bottom)

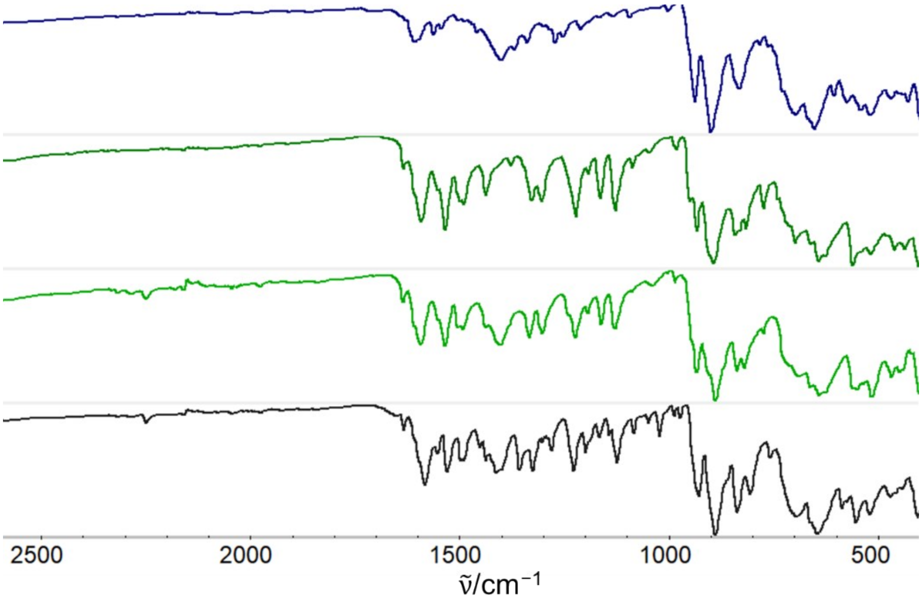

Figure S24. Comparison of IR-ATR spectra of **1**$^{\mathbf{Ow}}$, **2**$^{\mathbf{Ow}}$·10H_2O, **2**$^{\mathbf{Ow\text{-}2}}$·4MeCN·2H_2O and **4**$^{\mathbf{Ow\text{-}2}}$ ·2MeCN·3H_2O (from top to bottom)

Additional experimental details

A detailed description of the synthetic procedures for the synthesis of POM-based hybrids

Synthesis of hexamolybdate-based hybrids

$[MoO_2(HL^1)(H_2O)]_2[Mo_6O_{19}]$ ($\mathbf{1}^{\mathbf{Hw}}$). Hydrazone H_2L^1 (0.2 mmol) was added to a solution of $[MoO_2(acac)_2]$ (0.65 g; 2.0 mmol) in a mixture of 80 mL acetonitrile and 200 μL of acetic acid. The reaction mixture was stirred at room temperature for 3 hours and left overnight. The precipitated orange-brown solid was removed by filtration and the clear solution was left at room temperature. Slow crystallization yielded crystals of $\mathbf{1}^{\mathbf{Hw}}$ within two weeks. They were filtered, and transferred into a desiccator and placed overnight in a freezer (at −15 °C).

$[MoO_2(HL^2)(MeCN)]_2[Mo_6O_{19}]\cdot 4MeCN$ ($\mathbf{2}^{\mathbf{Hm}}\cdot 4MeCN$). Hydrazone H_2L^2 (0.2 mmol) was added to a solution of $[MoO_2(acac)_2]$ (0.65 g; 2.0 mmol) in a mixture of 80 mL acetonitrile and 200 μL of acetic acid. The reaction mixture was stirred at room temperature for 3 hours and left overnight. The precipitated orange-brown solid was removed by filtration, and the clear solution was left at room temperature. Slow crystallization yielded crystals of $\mathbf{2}^{\mathbf{Hm}}\cdot 4MeCN$ within two weeks. They were filtered, and transferred into a desiccator and placed overnight in a freezer (at −15 °C).

$[Mo_2O_2(\mu\text{-}O)_2(HL^3)_2][Mo_6O_{19}]$ ($\mathbf{3}^{\mathbf{H}}$). A mixture of $[MoO_2(acac)_2]$ (0.14 g, 0.430 mmol), hydrazone H_2L^3 (0.043 mmol), in acetonitrile were placed in 30 mL Teflon-lined autoclave and heated at 110 °C under autogenous pressure for three hours. Crystals of $\mathbf{3}^{\mathbf{H}}$ were obtained overnight. They were filtered and dried at ambient conditions.

$[MoO_2(HL^4)(H_2O)]_2[Mo_6O_{19}]\cdot 4MeCN$ ($\mathbf{4}^{\mathbf{Hw}}\cdot 4MeCN$). Hydrazone H_2L^4 (0.2 mmol) was added to a solution of $[MoO_2(acac)_2]$ (0.65 g; 2.0 mmol) in a mixture of 80 mL acetonitrile and 200 μL of acetic acid. The reaction mixture was stirred at room temperature for 3 hours and left overnight. The precipitated orange-brown solid was removed by filtration, and the clear solution was left at room temperature. Slow crystallization yielded crystals of $\mathbf{4}^{\mathbf{Hw}}\cdot 4MeCN$ within two weeks. They were filtered, and transferred into a desiccator and placed overnight in a freezer (at −15 °C).

Synthesis of octamoybdate-based hybrids

$[MoO_2(HL^1)(H_2O)]_4[Mo_8O_{26}]\cdot 2MeCN\cdot 4H_2O$ ($\mathbf{1}^{\mathbf{Ow}}\cdot 2MeCN\cdot 4H_2O$). Hydrazone H_2L^1 (0.2 mmol) was added to a solution of $[MoO_2(acac)_2]$ (0.65 g; 2.0 mmol) in a mixture of 40 mL acetonitrile and 100 μL of acetic acid. The reaction mixture was stirred at room temperature for 3 hours and left overnight. The precipitated solid was removed by filtration, and the clear solution was left at room temperature. The reaction mixture was filtered after two to three weeks, and the solution was left to slowly evaporate for further crystallization. This afforded crystals of $\mathbf{1}^{\mathbf{Ow}}\cdot 2MeCN\cdot 4H_2O$, after one month.

$[MoO_2(HL^2)(H_2O)]_4[Mo_8O_{26}]\cdot 2MeCN\cdot 10H_2O$ ($\mathbf{2}^{\mathbf{Ow}}\cdot 2MeCN\cdot 10H_2O$).
Hydrazone H_2L^2 (0.2 mmol) was added to a solution of $[MoO_2(acac)_2]$ (0.65 g; 2.0 mmol) in a mixture of 40 mL acetonitrile and 100 μL of acetic acid. The reaction mixture was stirred at room temperature for 3 hours and left overnight. The precipitated orange-brown solid was removed by filtration, and the clear solution was left at room temperature The reaction mixture was filtered after two weeks, and the solution was left to slowly evaporate for further crystallization. This afforded crystals of $\mathbf{2}^{\mathbf{Ow}}\cdot 2MeCN\cdot 10H_2O$, after one month.

$[MoO_2(H_2L^{2})(H_2O)]_2[Mo_8O_{26}]\cdot 4MeCN\cdot 2H_2O$ ($\mathbf{2}^{\mathbf{Ow\text{-}2}}\cdot 4MeCN\cdot 2H_2O$).
Hydrazone H_2L^2 (0.2 mmol) was added to a solution of $[MoO_2(acac)_2]$ (0.65 g; 2.0 mmol) in a mixture of 80 mL acetonitrile and 200 μL of acetic acid. The reaction mixture was stirred at room temperature for 3 hours and left overnight. The precipitated orange-brown solid was removed by filtration, and the clear solution was left at room temperature. The reaction mixture was filtered after two weeks, and the solution was left to slowly evaporate for further crystallization. This afforded $\mathbf{2}^{\mathbf{Ow\text{-}2}}\cdot 4MeCN\cdot 2H_2O$, after one month.

$[MoO_2(H_2L^{4})(H_2O)]_2[Mo_8O_{26}]\cdot 2MeCN\cdot 3H_2O$ ($\mathbf{4}^{\mathbf{Ow\text{-}2}}\cdot 2MeCN\cdot 3H_2O$).

Hydrazone H_2L^4 (0.2 mmol) was added to a solution of $[MoO_2(acac)_2]$ (0.65 g; 2.0 mmol) in a mixture of 80 mL acetonitrile and 200 μL of acetic acid. The reaction mixture was stirred at room temperature for 3 hours and left overnight. The precipitated orange-brown solid was removed by filtration, and the clear solution was left at room temperature. The reaction mixture was filtered after two weeks, and the solution was left to slowly evaporate for further crystallization. This afforded crystals of $\mathbf{4}^{\mathbf{Ow\text{-}2}}\cdot 2MeCN\cdot 3H_2O$, after one month.

$[MoO_2(H_2L^{4})(H_2O)]_2[Mo_8O_{26}]\cdot 3MeCN\cdot 4H_2O$ ($\mathbf{4}^{\mathbf{Ow\text{-}2}}\cdot 3MeCN\cdot 4H_2O$).

Hydrazone H_2L^4 (0.2 mmol) was added to a solution of $[MoO_2(acac)_2]$ (0.46 g; 1.40 mmol) in a mixture of 80 mL acetonitrile and 200 μL of acetic acid. The reaction mixture was stirred at room temperature for 3 hours and left overnight. The precipitated orange-brown solid was removed by filtration, and the clear solution was left at room temperature. The reaction mixture was filtered after two weeks, and the solution was left to slowly evaporate for further crystallization. This afforded crystals of $\mathbf{4}^{\mathbf{Ow\text{-}2}}\cdot 3MeCN\cdot 4H_2O$, after one month.

Experimental details and the overview of the products obtained depending on the starting compounds' molar ratio

The overview of all the product types depicted in Scheme 2 is given based on the following experimental results:

Hydrazone $H_2L^{1\text{-}4}$ (0.2 mmol) was added to a solution of $[MoO_2(acac)_2]$ (0.7 mmol, 1.4 mmol, or 2.0 mmol) in a mixture of 80 mL acetonitrile and 200 µL of acetic acid. The reaction mixture was stirred at room temperature for 3 hours and left overnight. The precipitated orange-brown solid was removed by filtration, and the clear solution was left at room temperature. Slow crystallization yielded crystals of **1**$^{\mathbf{Hw}}$, **2**$^{\mathbf{Hm}}$·4MeCN, **3**$^{\mathbf{Hw}}$, or **4**$^{\mathbf{Hw}}$·4MeCN within two weeks. They were filtered, and the solution was left for slow evaporation at room temperature. This afforded the corresponding octamolybdate-based hybrids **1**$^{\mathbf{Ow}}$·2MeCN·4H_2O, **2**$^{\mathbf{Ow}}$·2MeCN·10H_2O, **2**$^{\mathbf{Ow\text{-}2}}$·4MeCN·2H_2O or **4**$^{\mathbf{Ow\text{-}2}}$·2MeCN·H_2O after one to two months.

(1) By using the molar ratio 1:3.5, the first precipitate of $[MoO_2(L^{1\text{-}4})]_n$, was obtained in the yield 50-60%; the Lindqvist-based hybrids **1**$^{\mathbf{Hw}}$, **2**$^{\mathbf{Hm}}$·4MeCN, **3**$^{\mathbf{Hw}}$, and **4**$^{\mathbf{Hw}}$·4MeCN, crystalized after two weeks, yield: 15-20%.

(2) By using the molar ratio 1:7, the first precipitate of $[MoO_2(L^{1\text{-}4})]_n$, was obtained in the yield 20-30%; the Lindqvist-based hybrids **1**$^{\mathbf{Hw}}$, **2**$^{\mathbf{Hm}}$·4MeCN **3**$^{\mathbf{Hw}}$, **4**$^{\mathbf{Hw}}$·4MeCN, crystalized after two weeks (yield: in the range 35-50%), and the octamolybdate-based hybrids $[MoO_2(HL)(H_2O)]_4[Mo_8O_{26}]$ (**1**$^{\mathbf{Ow}}$·2MeCN·4H_2O and **2**$^{\mathbf{Ow}}$·2MeCN·10H_2O), and $[MoO_2(H_2L)(H_2O)]_2[Mo_8O_{26}]$ (**2**$^{\mathbf{Ow\text{-}2}}$·4MeCN·2H_2O, and **4**$^{\mathbf{Ow\text{-}2}}$·3MeCN·4H_2O) after one to two months, yield: 1-2%.

(3) By using the molar ratio 1:10, the first precipitate of $[MoO_2(L^{1\text{-}4})]_n$, was obtained in the yield up to 10%; the Lindqvist-based hybrids (**1**$^{\mathbf{Hw}}$, **2**$^{\mathbf{Hm}}$·4MeCN **3**$^{\mathbf{Hw}}$, **4**$^{\mathbf{Hw}}$·4MeCN), crystalized after two weeks (yield in the range 40-65%), and the octamolybdate-based hybrids $[MoO_2(HL)(H_2O)]_4[Mo_8O_{26}]$ (**1**$^{\mathbf{Ow}}$·2MeCN·4H_2O and **2**$^{\mathbf{Ow}}$·2MeCN·10H_2O), and $[MoO_2(H_2L)(H_2O)]_2[Mo_8O_{26}]$ (**2**$^{\mathbf{Ow\text{-}2}}$·4MeCN·2H_2O and **4**$^{\mathbf{Ow\text{-}2}}$·2MeCN·3H_2O) after one to two months, yield: 1-3%.